Journal of Medicinal Chemistry

Article

Synthesis of Piperlongumine Analogues and Discovery of Nuclear Factor Erythroid 2-Related Factor 2 (Nrf2) Activators as Potential Neuroprotective Agents

Shoujiao Peng, Baoxin Zhang, Xianke Meng, Juan Yao, and Jianguo Fang

J. Med. Chem., **Just Accepted Manuscript** • DOI: 10.1021/acs.jmedchem.5b00410 • Publication Date (Web): 16 Jun 2015

Just Accepted

Journal of Medicinal Chemistry is published by the American Chemical Society. 1155 Sixteenth Street N.W., Washington, DC 20036

Synthesis of Piperlongumine Analogues and Discovery of Nuclear Factor Erythroid 2-Related Factor 2 (Nrf2) Activators as Potential Neuroprotective Agents

Shoujiao Peng[#], Baoxin Zhang[#], Xianke Meng, Juan Yao, Jianguo Fang*

State Key Laboratory of Applied Organic Chemistry and College of Chemistry and Chemical Engineering, Lanzhou University, Lanzhou 730000, China

[#] These authors contribute equally to this work.

*Corresponding author, E-mail: fangjg@lzu.edu.cn (J. Fang); Fax: +86 931 8915557.

ABSTRACT

The cellular antioxidant system plays key roles in blocking or retarding the pathogenesis of adult neurodegenerative disorders as elevated oxidative stress has been implicated in the pathophysiology of such diseases. Molecules with the ability in enhancing the antioxidant defense thus are promising candidates as neuroprotective agents. We reported herein the synthesis of piperlongumine analogues and evaluation of their cytoprotection against hydrogen peroxide- and 6-hydroxydopamine-induced neuronal cell oxidative damage in the neuron-like PC12 cells. The structure-activity relationship was delineated after the cytotoxicity and protection screening. Two compounds (**4** and **5**) displayed low cytotoxicity and confer potent protection of PC12 cells from the oxidative injury via upregulation of a panel of cellular antioxidant molecules. Genetically silencing the transcription factor Nrf2, a master regulator of the cellular stress responses, suppresses the cytoprotection, indicating the critical involvement of Nrf2 for the cellular action of compounds **4** and **5** in PC12 cells.

INTRODUCTION

A small part of oxygen is continuously metabolized to reactive oxygen species (ROS) in aerobic cells under physiological conditions. The production of ROS and their synchronous elimination by an array of cellular antioxidant mechanisms are fundamental in maintaining the cellular redox homeostasis, which is pivotal for the regulation of diverse cellular functions, such as differentiation, proliferation, and death, via the activation or inactivation of transcription factors, metabolic enzymes, and membrane channels and so on.[1-3] Oxidative stress, arising from an increase of the ROS production and/or a simultaneous impairment of the cellular antioxidant capacity, causes deleterious effects and oxidative damage to various biomolecules, such as lipids, proteins, and nucleic acids, and ultimately leads to many pathophysiological conditions. Neurodegenerative disorders share many pathological features, such as accumulation of aberrant protein aggregates, microglial activation and mitochondrial dysfunction, all of which are associated with the elevated oxidative stress.[4] As neuronal cells are particular vulnerable to oxidative stress and have limited replenishment during entire lifespan, increasing lines of evidence have suggested oxidative stress as one of pathogenic causes in the neuropathology of adult neurodegenerative disorders such as Alzheimer's disease and Parkinson's disease.[4, 5] Supplementation of antioxidants or stimulation of cellular endogenous antioxidant defense system could efficiently block or retard the process of such diseases.[6, 7] Compared to the supplementation of exogenous antioxidants, the induction of endogenous antioxidant defense is preferred as such action is more sustainable and regulated at transcriptional level.

The Nrf2 (nuclear factor erythroid 2-related factor 2) transcription factor plays a critical role in cellular stress response and its malfunction is involved in a number of disease processes.[8, 9] In

unstressed cells, Nrf2 forms a complex with the inhibitory protein Kelch-like ECH-associated protein 1 (Keap1), which anchors Nrf2 in cytosol and directs it to ubiquitin-mediated proteasome degradation.[10] The association of Keap1 with Nrf2 relies on the active sulfhydryl group of cysteine residue(s) in the protein Keap1. Stimulants, such as electrophiles and oxidants, that could modify such cysteine residue(s) cause the dissociation of Nrf2 from the Keap1, hence increasing Nrf2 stability and further facilitating Nrf2 to translocate into nucleus, where Nrf2 binds to a common DNA sequence called antioxidant response elements (ARE) to initiate the transcription of a panel of cytoprotective genes (phase II genes).[9] As a global regulator of cellular antioxidant responses, Nrf2 controls a majority of antioxidants pathways, including the production of cellular universal reducing equivalent NADPH, the synthesis, utilization and regeneration of glutathione (GSH), the expression of thioredoxin system, and the synthesis of heme oxygenase-1 (HO-1) and NAD(P)H quinone oxidoreductase 1 (NQO1). In this sense, activation of Nrf2-ARE pathway is a promising therapeutic approach in treatment of neurodegenerative disorders,[11, 12] and thus the past years have witnessed the expanding interests in identifying and developing naturally occurring or synthetic small molecule activators of Nrf2-ARE pathway as potential neuroprotective agents.[6, 13-16]

Natural products and their synthetic derivatives are invaluable fountain for therapeutic agents, and have driven pharmaceutical discovery over the past century. Piperlongumine (PL, Fig. 1) is a naturally occurring alkaloid from the plant Long pepper (*Piper longum*), which has long been used as a fold medicine as well as spicy food additive. PL has been documented having multiple pharmacological activity,[17] such as anti-platelet aggregation,[18] anti-inflammation[19] and cardiovascular protection.[20] The discovery that PL induces cell death preferentially in cancer cells via elevation of cellular ROS levels turns the page for considering treatment of cancers with PL.[21]

Since then, diverse analogues of PL have been prepared to find novel compounds with improved properties.[22-25] Although increasing attention has been devoted to the biological functions of PL and its synthetic analogues, there is no study on the neuroprotection of PL. We reported herein the synthesis and evaluation of PL and its analogues as potential neuroprotective agents against oxidative stress-mediated cell damage in a neuron-like cell line, PC12 cells. Most of the PL analogues display remarkable protection of PC12 cells against hydrogen peroxide- or 6-hydroxydopamine (6-OHDA)-induced cell injury. Two compounds (**4** and **5**) were chosen for the follow-up studies as they possess lower cytotoxicity and better protection. Hydrogen peroxide or 6-OHDA induces ROS accumulation and apoptosis in PC12 cells, which could be efficiently suppressed by the pretreatment of the cells with **4** or **5**. Mechanistic studies reveal that both compounds are potent Nrf2 activators to promote the nuclear translocation of Nrf2, which facilitates the expression of a series of Nrf2-driven antioxidant molecules, including HO-1, NQO1, GSH, thioredoxin 1 (Trx1) and thioredoxin reductase 1 (TrxR1). In addition, knockdown of Nrf2 by shRNA transfection abolishes the cytoprotection, demonstrating that activation Nrf2 is the molecular mechanism underlying the cellular action of compounds **4** and **5** in PC12 cells.

RESULTS AND DISCUSSION

Chemical synthesis. PL and its analogues were synthesized by a convergent strategy that entails coupling commercially available or synthetically accessible lactams and carboxylic acid chlorides (Scheme 1) according to the published procedures.[22, 23, 25-27] All compounds were fully characterized by ^{1}H, ^{13}C NMR and MS, and their structures were illustrated in Fig. 1. The purity of PL and its synthetic analogues was determined by the HPLC analysis, and was greater than 95%.

Initial screening. The cytotoxicity of all compounds towards the PC12 cells and L02 cells (an immortal hepatic cell line) were determined by the MTT assay. As shown in Fig. 2A, PL, among all the tested compounds, displays the highest toxicity towards PC 12 cells. Compounds **9-18** also give significant toxicity to the cells at high concentration (100 μM), while compounds **2-8**, and **19** only show marginal effect on the growth of the cells. The cytotoxicity of the compounds follows a similar trend in the L02 cells (Fig. 2B): PL~**9-14**>**15-18**>**2-8**, **19**. Except PL, there is no apparent toxicity of the tested compounds towards the PC12 cells at 20 μM. Next, we determined the protection of compounds **2-19** against the H_2O_2- and 6-OHDA-induced PC12 cell damage, two well-established cellular models of neurodegenerative disorders.[13, 14, 28] All the tested compounds, except **7**, are capable of relieving the cell injury. Notably, **4** and **5** give the better protection (Fig. 3).

Protection of PC12 cells from H_2O_2- and 6-OHDA-induced damage by 4 and 5. As compounds **4** and **5** display lower cytotoxicity (Fig. 2) and better protection (Fig. 3) in the initial screening, we then selected these two compounds for the follow-up studies. As shown in Fig. 4A, PC12 cells treated with H_2O_2 only showed about half cell death compared with the control group. However, if the cells were pretreated with **4** or **5** (10 or 20 μM) for 24 h followed by H_2O_2 insult, the population of viable cells increased remarkably in dose-dependent manners. Compounds **4** and **5**

(20 μM) increased the cell viability to ~75% and ~80%, respectively. 6-OHDA is a potent neurotoxin, and widely used to generate an experimental model of Parkinson's disease. 6-OHDA-mediated neurotoxicity is engendered, at least in part, by its ability to generate ROS.[29] As shown in Fig. 4B, 6-OHDA reduced cell viability to about 50 % of the control. Similarly, addition of **4** or **5** also markedly promoted cell viability to ~75 % (Fig. 4B). Lactate dehydrogenase (LDH) is a soluble cytosolic enzyme that is released into the culture medium following loss of membrane integrity resulting from cell damage. To confirm the cytoprotection of compounds **4** and **5**, we further determined the content of LDH leakage after H_2O_2 or 6-OHDA insult. As shown in Fig. 4C & D, H_2O_2 and 6-OHDA cause ~2.2-fold and ~1.8-fold increase of LDH release, respectively. Pretreatment of PC12 cells with **4** or **5** significantly reduces the leakage of LDH. Taken together, compounds **4** and **5** at non-toxic concentration can significantly protect PC12 cells from H_2O_2- or 6-OHDA-induced cell injury.

Alleviation of H_2O_2- and 6-OHDA-induced PC12 cell apoptosis. Nuclear chromatin condensation and cytosolic caspases activation are hallmarks of cell apoptosis. The morphologic changes of the nuclei were revealed by the Hoechst staining assay. Hoechst dyes are a family of blue fluorescent molecules used to stain DNA. Hoechst 33342 is a popular cell-permeant dye that emits strong blue fluorescence when bound to double strand DNA, and is widely applied to distinguish condensed pycnotic nuclei in apoptotic cells.[13, 14, 30-33] As shown in Fig. 5A & 5B, both H_2O_2 and 6-OHDA elicit apoptosis in PC12 cells evidenced by the appearance of the characteristic apoptotic nuclei as highly fluorescent, condensed bodies (indicated by arrows), while no apparent apoptotic nuclei were observed in the control cells. Pretreatment of the cells with non-toxic concentrations of **4** or **5** remarkably decreases the population of apoptotic nuclei. Next, we

measured the caspase-3 activity in PC12 cells. Both H_2O_2 and 6-OHDA activate the cellular caspase-3 (Fig. 5C & 5D). Again, compounds **4** and **5** efficiently alleviate the extent of caspase-3 activation in a concentration–dependent manner. Collectively, these results indicate that compounds **4** and **5** could assuage the H_2O_2- and 6-OHDA-induced PC12 cell apoptosis.

Prevention of ROS accumulation in PC12 cells. 2',7'-dichlorfluorescein diacetate (DCFH-DA) is a cell-permeable, non-fluorescent dye. After diffusing into cells, DCFH-DA is deacetylated by cellular esterases to non-fluorescent 2',7'-dichlorodihydrofluorescin, which is rapidly converted to highly fluorescent 2',7'-dichlorofluorescein upon reacting with ROS. Stimulation of the cells with H_2O_2 or 6-OHDA leads to appearance of bright green fluorescence, indicating the burst of ROS in the cells. The control cells display negligible ROS level as they remain non-fluorescent (Fig. 6A & 6B). Pretreatment of the cells with **4** or **5** remarkably and dose-dependently reduces the ROS accumulation induced by either H_2O_2 or 6-OHDA. Oxidative stress, arising from the overproduction of ROS beyond the cellular antioxidant capacity to remove them, has been implicated in a common pathway of neurotoxicity in a wide variety of acute and chronic neurologic disorders. Prevention of ROS accumulation in neuronal cells by compounds **4** and **5** might account for their cytoprotection against oxidative injury.

Induction of antioxidant genes expression. To further study the role(s) of **4** and **5** in releasing the ROS stress imposed by H_2O_2 or 6-OHDA in PC12 cells (Fig. 6), we then determined their direct free radical scavenging activity. Compounds **4** and **5** are incapable of intercepting either 2,2-diphenyl-1-picrylhydrazyl (DPPH) or 2,2′-azinobis-(3-ethylbenzothiazoline-6-sulfonic acid) (ABTS) free radicals (Fig. S1 in the Supporting Information), indicating that **4** and **5** cannot act as direct radical scavengers. This may be understood by that the free radical-scavenging antioxidants

generally contain active functionalities, such as phenoxy group or/and sulfhydryl group, which easily donates electrons to free radicals via a hydrogen abstraction reaction or electron transfer reaction. However, compounds **4** and **5** don't have such active groups, and thus they cannot scavenge free radicals directly via chemical ways. In support of this, **19**, the demethylated derivative of **5**, efficiently neutralizes both radicals (Fig. S1 in the Supporting Information). Analysis of the structure of **4** and **5** reveals that they belong to the chalcone family, which bears α, β-unsaturated ketone structure. Due to the electron-deficient character of the double bond, this moiety is renowned as Michael acceptor, which is a core structure of many reported small molecule ARE inducers.[15] In analogy to the known ARE activators, we thus hypothesized that **4** and **5** might activate the cellular ARE response. We determined the expression of Nrf2-driven antioxidant/detoxifying genes (HO-1, Trx1, TrxR1, NQO1, GCLC and GCLM) at 0, 3, 6 and 12 h after treatment with **4** or **5** (20 μM) in PC12 cells (Fig. 7). Significant induction of all the tested genes was observed at 6 h. Among all the genes, Trx1 and TrxR1 are most notable as they were induced even at 3 h, and the induction of both genes is sustainable even after 12 h. Our data demonstrate that treatment of the PC12 cells with **4** and **5** effectively promotes the transcription of Nrf2-driven antioxidant/detoxifying genes.

Upregulation of the antioxidant defense system in PC12 cells. As a series of antioxidant genes has been up-regulated in PC12 cells after compounds **4** or **5** stimulation (Fig. 7), we then examined the corresponding gene products. The amount of GSH was quantified by the enzymatic assay as described in the Experimental section. The expression and function of antioxidant enzymes were determined by Western blots and activity assays, respectively. As shown in Fig. 8A, D, G, & J, compounds **4** and **5** remarkably elevates GSH level and antioxidant enzymes activity (NQO1, Trx

and TrxR). In the H_2O_2 or 6-OHDA injury model (Fig. 8B, C, E, F, H, I, K & L), the amount of GSH, and the activity of NQO1, Trx and TrxR were significantly impaired. Pretreatment of the cells with **4** or **5** could rescue both the GSH amount and the enzymes activity. The expression patterns of HO-1, NQO1, Trx1 and TrxR1 were illustrated in Fig. 8M, and all the proteins were upregulated, consistent with the elevation of their activity. We further confirmed the induction of TrxR activity in live PC12 cells by our recently developed probe, TRFS-green.[34] The increment of the green fluorescence indicated the boost of the TrxR activity (Fig. 8N).

Promotion of Nrf2 nuclear localization. Induction of transcription of antioxidant genes via the Nrf2-dependent cytoprotective pathway requires translocation of Nrf2 from cytosol to nucleus. We therefore examined whether **4** and **5** could promote the Nrf2 to accumulate in nuclei. After isolating the nuclei from the cells, the total Nrf2, the cytosolic Nrf2, and the nuclear Nrf2 were determined by immunoblots. Upon **4** or **5** treatment, the immunoblotting results revealed that the total Nrf2 expression was slightly upregulated (Fig. 9, bottom panel). Notably, the cytosolic Nrf2 decreased gradually (Fig. 9, middle panel). Coincidently, the amount of Nrf2 in nuclei increased (Fig. 9, top panel), indicating the translocation of Nrf2 from the cytosol to the nuclei. The presence of Nrf2 in nuclei would facilitate its binding to ARE, and thus subsequently initiates the transcription process to induce the antioxidant genes expression.

Requirement of Nrf2 for the cytoprotection of 4 and 5. We further asked the role of Nrf2 for the cellular protection of **4** and **5** in response to oxidative insults. For this purpose, we transfected the cells with the shRNA plasmid specifically targeting the Nrf2 to generate stable transformants of PC12 cells silencing the expression of Nrf2 (PC12-shNrf2 cells). As a control, PC12 cells were also transfected with a non-targeting shRNA to afford the control cells

(PC12-shNT cells). After confirming the knockdown efficiency of Nrf2 by Western blots (Fig. 10A), we evaluated the effect of **4** and **5** against oxidative challenge toward different cells. As shown in Fig. 10B & C, compounds **4** and **5** display the similarly protective pattern in PC12-shNT cells as that observed in wild type PC12 cells. However, this protection is almost completely suppressed in PC12-shNrf2 cells, demonstrating the definite involvement of Nrf2 for the cytoprotection of **4** and **5** in PC12 cells.

Medicinal chemical properties of compounds 4 and 5. The medicinal chemical properties of a molecule could predict whether it is capable of passing the blood-brain barrier (BBB). The general criteria for a compound to cross the BBB are as the follows:[35] the molecular weight (MW) is less than 450, cLogP is between 0 and 5, and the polar surface area (PSA) is less than 70 $Å^2$. The values of cLogP, PSA and MW of compounds **4** and **5** were summarized in Table 1. By determination of the partition coefficient between *n*-octanol and water, the cLogP values were obtained. The positive control *o*-cresol gives a value of 1.95, consistent with the data in the reference (1.98 ± 0.05).[36] Thus, the medicinal chemical properties of compounds **4** and **5** suggest they have the ability to penetrate the BBB for a potential CNS drug.

ROS are physiological metabolites from numerous cellular processes in all aerobes.[1, 37] Low levels of ROS are signaling molecules to promote proliferation and survival pathways.[38] However, high levels of ROS exert an oxidative stress on the cell that damages various cellular components, such as lipids, proteins and DNA, and ultimately cause cell senescence or death.[38, 39] Common potential targets and putative mechanisms of neurodegenerative diseases have been elegantly summarized in the recent Perspective.[6] Although the molecular mechanism underlying the

pathogenesis of neurodegeneration is still in debate, increasing evidence has supported that oxidative stress is a causal, or at least an ancillary, factor in the progressive degeneration of a subset of neurons, which is the pathologic hallmark of adult-onset neurodegenerative disorders.[7, 40] The incapability of the adult human brain to regenerate and the limited success of the surgical operation to replace the lost or damaged neurons have led to intense efforts to explore the pharmacological management aiming to suppress the oxidative stress, which is expected eventually leading to retardation or blockage of the neurodegenerative progression. As a master regulator of the cellular antioxidant responses, the transcription factor Nrf2 has appeared as an emerging drug target to counteract the oxidative stress-mediated pathogenic processes.[12, 15] The observation that genetic activation of Nrf2 signaling efficiently ameliorates neurodegenerative phenotypes in a fly model of Parkinson's disease further supports the therapeutic potential of Nrf2.[41]

Preceding studies have indicated that PL and its analogues have a number of pharmacological functions.[17-21, 42] However, the neuroprotective function of PL has not been investigated prior to this report. Molecules with *ortho*-diphenoxyl groups or/and Michael acceptor units appear to potential Nrf2 activators to induce various endogenous antioxidant and detoxifying molecules.[13, 14, 43] PL contains two Michael acceptor units (highlighted as M1 and M2 in Fig. 1), suggesting that PL might be promising for cytoprotection. However, the high cytotoxicity of PL hinders its application as a cytoprotective agent.[21] As our continued interests in discovering and developing novel redox active small molecules as potential therapeutic or diagnostic agents,[30, 32, 34, 44-47] we described the synthesis of PL and its analogues, and the discovery of two potent compounds (**4** and **5**) as potential neuroprotective agents to rescue the H_2O_2- or 6-OHDA-induced PC12 cell damage. Compared to the cytotoxicity data of **4** (a compound lacking the M2 moiety), PL shows greater toxic to both L02

cells and PC12 cells. These results are consistent with the previous report that M2 is critical for the cytotoxicity of PL.[25] As the goal of this study is to seek potential neuroprotective agents, a set of PL analogues without the M2 were prepared to minimize the cytotoxicity of the compounds. Based on the initial cytotoxicity and protection screening results (Figures 2 & 3), the preliminary structure-activity relationship (SAR) could be drawn: 1) The Michael acceptor within the lactam ring (M2) is responsible for the cytotoxicity as PL shows higher cytotoxicity than **4**, while the M1 is required for the cytoprotection as all analogues except N7 are capable of rescuing the cells from oxidative damage; 2) Introducing the electron-withdrawing groups (EWG) to the benzene ring, such as **9-15**, generally increase the cytotoxicity, while introducing the electron-donating groups, such as **2-6** and **8**, decreases the cytotoxicity; 3) The ring size of the lactam appears no apparent effect on the protective potency or cytotoxicity as the compounds **2**, **4** and **8,** and the compounds **16-18** exhibit indiscriminate activity. The SAR disclosed here will guide the further modification of PL with improved biological functions.

Our results demonstrated that compounds **4** and **5** displayed potent cytoprotection against H_2O_2- or 6-OHDA-induced neuronal cell damage in PC12 cells via the induction of phase II antioxidant/detoxifying enzymes. Treatment of PC12 cells with **4** or **5** at nontoxic concentrations promotes nuclear translocation of the transcription factor Nrf2, and subsequently upregulates a set of Nrf2-driven genes as well as the corresponding gene products, including the antioxidant enzymes (HO-1, NQO1, Trx1, and TrxR1) and small peptide antioxidant GSH. The elevation of cellular endogenous antioxidant system prevents the accumulation of ROS, and thus confers protection against oxidative insults to the cells. Knockdown of Nrf2 expression almost completely deprives the protection, supporting the physiological significance of targeting Nrf2 by **4** and **5** in PC12 cells. The

clarification of the cellular target and the action mechanism would provide information for the further development of PL analogues as potential therapeutic drugs. One major challenge for most neuroprotective agents in vivo is their ability to pass through the blood-brain barrier (BBB). The recent study disclosed that PL could cross the BBB after oral administration.[48] The small size (PSA<70 and MW<450), non-polar character (cLogP<5) and similar structure with PL would favor both compounds to penetrate the BBB. It is much like that **4** and **5** has the ability to pass through the BBB in vivo.

The Michael acceptor moieties, notorious for the electrophilic property which gives them promiscuous reactivity towards various electron-rich biomolecules, were generally excluded in the traditional drug design process. However, accumulating evidence has supported that Michael acceptors are promising pharmacophores for cytoprotective drugs as molecules bearing such functionalities are effective activators of Keap1-Nrf2-ARE pathway.[28, 49, 50] The recently FDA-approved drug dimethyl fumarate (BG-12, a Michael acceptor) for multiple sclerosis consolidates this concept.[51] We previously reported that several natural products bearing α, β-unsaturated ketone structure (a Michael acceptor moiety), such as xanthohumol and 6-dehydrogingerdione,[13, 14] are potent Nrf2 activators to afford neuroprotection in cellular models. Compounds **7**, a compound similar to **4** but lacking the Michael acceptor unit, has little protection, indicating the importance of the α, β-unsaturated amide structure for the cellular action of PL analogues. In analogy to the activation of Nrf2 by xanthohumol[13] and 6-dehydrogingerdione,[14] we reasoned that bind of the compounds via their Michael acceptor moiety to the cysteine residue(s) in the inhibitory protein Keap1 might be the molecular basis for the activation of Nrf2.

CONCLUSIONS

In summary, a series of PL analogues has been synthesized, and two PL analogues, *i. e.*, **4** and **5**, have been identified as potent Nrf2 activators with minimal cytotoxicity. Compounds **4** and **5** promote Nrf2 nuclear translocation, and hence facilitate transcription of a variety of cytoprotective genes, conferring protection of PC12 cells against oxidative insults. The clarification of the cellular target, the action mechanism and the structural determents for the activity of **4** and **5** would guide the further development of PL analogues as potential therapeutic drugs.

EXPERIMENTAL PROCEDURES

Materials. Dulbecco's modified Eagle's medium (DMEM), N-acetyl-Asp-Glu-Val-Asp-p-nitroanilide (Ac-DEVD-pNA), dimethyl sulfoxide (DMSO), yeast glutathione reductase (GR), Hoechst 33342, DCFH-DA, 5,5'-dithiobis-2-nitrobenzoic acid (DTNB), AAPH, DPPH, 2,6-dichlorophenol-indophenol (DCPIP), NADH, 3-(4, 5-dimethylthiazol-2-yl)-2, 5-diphenyltetrazolium bromide (MTT), 2,2'-azinobis(3-ethylbenzthiazoline-6- sulfonic acid (ABTS), 2, 2-diphenyl-1-picrylhydrazyl (DPPH), penicillin and streptomycin were obtained from Sigma-Aldrich (St. Louis, USA). NADPH was obtained from Roche (Mannheim, Germany). Fetal bovine serum (FBS) was obtained from HyClone. 6-OHDA, hydrogen peroxide, antibodies against TrxR1 and Nrf2 were from Santa Cruz Biotechnology. Antibodies against HO-1, NQO1 and Trx1 were from Sangon Biotech (Shanghai, China). The shRNA plasmids targeting coding regions of the rat Nrf2 gene (shNrf2) and the control non-targeting shRNA (shNT) were purchased from Gene Pharma Co, Ltd (Shanghai, China). GeneTran III transfection reagent was obtained from Biomiga (CA, USA). Bovine serum albumin (BSA), phenylmethanesulfonyl fluoride (PMSF), sodium

orthovanadate (Na_3VO_4), and anti-lamin and anti-actin antibodies were from Beyotime (Nantong, China). The recombinant rat TrxR1 is a gift from Prof. Arne Holmgren at Karolinska Institute. The recombinant *E. coli* Trx was prepared according to our published procedures.[31] All other reagents were of analytical grade.

Compounds Purity Analysis. PL and its analogues were analyzed by HPLC to determine their purity. The analyses were performed on Waters 1525 2998 series HPLC system (C-18 column, Sun Fire, 5 μm, 4.6 mm×150 mm) at room temperature. The HPLC chromatograms of compounds **1-19** were included in the Supporting Information (Fig. S2-S6). All the tested compounds were dissolved in methanol, and 10 μL of the sample was loaded onto the column. Methanol and water were used as mobile phase, and the flow rate was set at 1.0 mL/min. The maximal absorbance at the range of 210-400 nm was used as the detection wavelength. The purity of all the tested compounds (compounds **1-19**) is >95%, which meets the purity requirement by the Journal.

Chemical Synthesis. The detailed starting materials and synthetic intermediates in the Scheme 1 were summarized in Table S1 in the Supporting Information.

Synthesis of substituted cinnamic acids (Step a in Scheme 1).[27, 52, 53] Malonic acid (0.3 g, 2.86 mmol) was added to the stirred solution of the corresponding aldehyde (1.3 mmol) in pyridine (15 mL) and piperidine (1.5 mL). The mixture was heated to reflux for 8 h. The reaction mixture was neutralized with hydrochloric acid in an ice bath. The white precipitates were filtered and washed with cold water. The crude products were recrystallized from aqueous ethanol to afford the corresponding acids.

Synthesis of substituted cinnamic acid chlorides (Step b in Scheme 1).[54] To a solution of acids (1.0 mmol) in dry CH_2Cl_2 was added oxalyl chloride (5.0 equiv.) and catalytic amount of DMF

(0.01 equiv.). The reaction mixture was stirred at room temperature for 5 h before the solvent was removed. The residue was dried under high vacuum, and used to the next step without any further purification.

Synthesis of PL and its analogues (Step c in Scheme 1).[25, 26] To a solution of acid chloride (1.0 equiv.) in CH_2Cl_2 were added triethylamine (TEA, 3.0 equiv.) and lactam (1.2 equiv.). The reaction mixture was stirred at room temperature overnight before it was quenched with saturated aqueous NH_4Cl, and extracted with CH_2Cl_2. The combined organic phases were washed with brine and dried over $MgSO_4$. After filtration and concentration, the residue was purified by flash chromatography to provide the desired amides.

*Synthesis of **7** (Step d in Scheme 1).* To a mixture of 100 mg of Pd/C (10 %) in 10 ml of ethyl acetate under a hydrogen atmosphere was added **4** (1.0 mmol). The reaction was kept at room temperature for 12 h. After the reaction completing, the Pd/C was removed by filtration, and the filtrate was concentrated and purified by silica gel column chromatography to afford **7**.

*(E)-1-(3-(3,4,5-Trimethoxyphenyl)acryloyl)-5,6-dihydropyridin-2(1H)-one (**1**).*[25] Yield: 25%. ^{1}H NMR (400 MHz, $CDCl_3$) δ: 7.72 (d, *J* = 15.6 Hz, 1H, Ar-CH=CH-), 7.41 (d, *J* = 15.6 Hz, 1H, Ar-CH=CH-), 6.80 (s, 2H, ArH_2), 6.58 (m, 1H, -CH=CH-), 6.13 (d, *J* = 11.6 Hz, 1H, -CH=CH-), 4.02 (t, 2H, -CH_2-), 3.90 (s, 6H, 2 -OCH_3), 3.88 (s, 3H, -OCH_3), 2.44(m, 2H, -CH_2-); ^{13}C NMR (100 MHz, $CDCl_3$) δ: 171.4, 167.6, 153.2, 144.1, 142.1, 139.9, 130.5, 127.9, 120.1, 105.45, 60.9, 56.1, 41.2, 26.1, 25.4; ESI-MS(m/z): $[M+H]^+$ 318.2; mp: 156-158 ^{o}C; purity: 95.21% (MeOH/H_2O = 70/30, R_t= 4.964 min).

*(E)-1-(3-(3,4,5-Trimethoxyphenyl)acryloyl)pyrrolidin-2-one (**2**).*[55] Yield: 45%. ^{1}H NMR (400 MHz, $CDCl_3$) δ: 7.87 (d, *J* = 15.6 Hz, 1H, Ar-CH=CH-), 7.78 (d, *J* = 15.6 Hz, 1H, Ar-CH=CH-),

6.84 (s, 2H, ArH_2), 3.96 (t, 2H, N-CH_2-),3.91 (s, 6H, 2 -OCH_3), 3.89 (s, 3H, -OCH_3), 2.69 (t, 2H, -$COCH_2$-), 2.13 (m, 2H, -CH_2-); ^{13}C NMR (100 MHz, $CDCl_3$) δ:175.8, 174.6, 166.2, 153.4, 152.7, 145.6, 140.2, 130.4, 118.2, 105.6, 60.9, 56.2, 45.9, 34.0, 17.2; ESI-MS(m/z): $[M+H]^+$ 306.3; mp: 152-154 ^{o}C; purity: 98.49% (MeOH/H_2O = 65/35, R_t= 4.335 min).

*(E)-1-(3-(3,4-Dimethoxyphenyl)acryloyl)pyrrolidin-2-one (**3**).*[56] Yield: 44%. ^{1}H NMR (400 MHz, $CDCl_3$) δ: 7.86 (d, *J* = 15.6 Hz, 1H, Ar-CH=CH-), 7.81 (d, *J* = 15.6 Hz, 1H, Ar-CH=CH-), 7.21 (dd, *J* = 8.4, 2.0 Hz, 1H, ArH), 7.14 (d, *J* = 1.6 Hz, 1H, ArH), 6.89 (d, *J* = 8.4 Hz, 1H, ArH) 3.94 (s, 6H, 2 -OCH_3), 3.93 (t, 2H, N-CH_2-), 2.68 (t, 2H, -$COCH_2$-), 2.12 (m, 2H, -CH_2-); ^{13}C NMR (100 MHz, $CDCl_3$) δ: 175.7, 166.4, 151.2, 149.1, 145.6, 127.9, 123.1, 116.6, 110.9, 109.9, 55.9, 55.8, 45.9, 34.0, 17.1; ESI-MS(m/z): $[M+H]^+$ 275.8; mp: 128-130 ^{o}C**;** purity: 95.95% (MeOH/H_2O = 65/35, R_t= 3.962 min).

*(E)-1-(3-(3,4,5-Trimethoxyphenyl)acryloyl)piperidin-2-one (**4**).*[25] Yield: 40%. ^{1}H NMR (400 MHz, $CDCl_3$) δ: 7.65 (d, *J* = 15.6 Hz, 1H, Ar-CH=CH-), 7.37 (d, *J* = 15.6 Hz, 1H, Ar-CH=CH-), 6.78 (s, 2H, ArH_2), 3.88 (s, 6H, 2 -OCH_3), 3.87 (s, 3H, -OCH_3), 3.81 (t, 2H, N-CH_2-), 2.63 (t, 2H, -$COCH_2$-), 1.90(m, 4H, -CH_2CH_2-); ^{13}C NMR (100 MHz, $CDCl_3$) δ: 173.9, 169.6, 153.3, 143.4, 139.7, 130.6, 121.3, 105.4, 60.9, 56.1, 44.6, 34.9, 22.5, 20.6; ESI-MS(m/z): $[M+H]^+$ 320.2; mp: 109-110 ^{o}C; purity: 99.88% (MeOH/H_2O = 65/35, R_t=4.941min).

*(E)-1-(3-(4-Methoxyphenyl)acryloyl)pyrrolidin-2-one (**5**).*[57] Yield: 55%. ^{1}H NMR (400 MHz, $CDCl_3$) δ: 7.84 (d, *J* = 16.0 Hz, 1H, Ar-CH=CH-), 7.80 (d, *J* = 16.0 Hz, 1H, Ar-CH=CH-), 7.57 (d, *J* = 8.8 Hz, 2H, ArH_2), 690 (d, *J* = 8.8 Hz, 2H, ArH_2), 3.92 (t, 2H, N-CH_2-), 3.82 (s, 3H, -OCH_3), 2.65 (t, 2H, -$COCH_2$-), 2.08 (m, 2H, -CH_2-); ^{13}C NMR (100 MHz, $CDCl_3$) δ: 175.6, 166.5, 161.4, 145.2, 130.2, 127.6, 116.4, 114.2, 55.3, 45.8, 34.0, 17.1; ESI-MS(m/z): $[M+H]^+$ 245.8; mp: 110-112 ^{o}C;

purity: 98.36% (MeOH/H_2O = 65/35, R_t= 5.744 min).

*(E)-1-(3-(4-Methoxyphenyl)acryloyl)piperidin-2-one (**6**).* Yield: 43%. ^{1}H NMR (400 MHz, $CDCl_3$) δ: 7.72 (d, *J* = 15.6 Hz, 1H, Ar-CH=CH-), 7.54 (d, *J* = 8.8 Hz, 2H, ArH_2), 7.38 (d, *J* = 15.6 Hz, 1H, Ar-CH=CH-), 6.90 (d, *J* = 8.4 Hz, 2H, ArH_2) , 3.84 (s, 3H, -OCH_3), 3.82 (t, 2H, N-CH_2-), 2.62 (t, 2H, -$COCH_2$-), 1.90 (m, 4H, -CH_2CH_2-); ^{13}C NMR (100 MHz, $CDCl_3$) δ: 173.8, 169.8, 161.1, 143.1, 129.9, 127.8, 119.6, 114.1, 55.3, 44.5, 34.9, 22.5, 20.5; ESI-MS(m/z): $[M+Na]^+$ 282.0; mp: 70-71 ^{o}C; purity: 98.40% (MeOH/H_2O = 70/30, R_t= 4.895 min).

*1-(3-(3,4,5-Trimethoxyphenyl)propanoyl)piperidin-2-one (**7**).*[25] Yield: 20%. ^{1}H NMR (400 MHz, $CDCl_3$) δ: 6.46 (s, 2H, ArH_2), 3.84 (s, 6H, 2 -OCH_3), 3.81 (s, 3H, -OCH_3), 3.72 (t, 2H, N-CH_2-), 3.24 (t, 2H, $ArCH_2$-), 2.93 (t, 2H, -CH_2CO-), 2.55 (t, 2H, -CH_2CO-),1.82 (t, 4H, -CH_2CH_2-); ^{13}C NMR (100 MHz, $CDCl_3$) δ: 176.0, 173.4, 137.0, 136.2, 105.4, 60.8, 56.0, 44.0, 41.3, 34.8, 31.5, 22.4, 20.2; ESI-MS(m/z): $[M+H]^+$ 322.3; mp: 75-76 ^{o}C; purity: 96.03% (MeOH/H_2O = 65/35, R_t= 4.582 min).

*(E)-1-(3-(3,4,5-Trimethoxyphenyl)acryloyl)azepan-2-one (**8**).* Yield:.40%. ^{1}H NMR (400 MHz, $CDCl_3$) δ: 7.65 (d, *J* = 15.2 Hz, 1H, , Ar-CH=CH-), 7.35 (d, *J* = 15.6 Hz, 1H, , Ar-CH=CH-), 6.79 (s, 2H, ArH_2), 3.99 (t, 2H, N-CH_2-),3.89 (s, 6H, 2-OCH_3), 3.88 (s, 3H, OCH_3), 2.27 (t, 2H, -$COCH_2$-), 1.84 (m, 6H, -$CH_2CH_2CH_2$-); ^{13}C NMR (100 MHz, $CDCl_3$) δ:178.1, 168.8, 153.2, 143.5, 139.9, 130.7, 121.2, 105.4, 60.9, 56.1, 43.8, 39.6, 29.2, 28.6, 23.7; ESI-MS(m/z): $[M+H]^+$ 334.2; mp: 92-93 ^{o}C; purity: 96.61% (MeOH/H_2O = 65/35, R_t= 6.753 min).

*(E)-1-(3-(4-(Trifluoromethyl)phenyl)acryloyl)pyrrolidin-2-one (**9**).*[58] Yield: 25%. 1H NMR (400 MHz, CDCl3) δ: 8.00 (d, J = 15.6 Hz, 1H, Ar-CH=CH-), 7.82 (d, J = 15.6 Hz, 1H, Ar-CH=CH-), 7.71 (d, J = 8.0 Hz, 2H, ArH_2), 7.64 (d, J = 8.0 Hz, 2H, ArH_2), 3.94 (t, 2H, N-CH_2-),

2.67 (t, 2H, -$COCH_2$-), 2.10 (m, 2H, -CH_2-); ^{13}C NMR (100 MHz, $CDCl_3$) δ: 176.0, 166.0, 143.5, 138.4, 132.1, 131.7, 128.8, 126.0, 125.9, 122.7, 121.7, 46.0, 34.1, 17.4; ESI-MS (m/z): [M + H^+] 283.8; mp: 126-128 ^oC; purity: 98.90% (MeOH/H_2O = 70/30, R_t= 7.635 min).

*(E)-1-(3-(4-Bromophenyl)acryloyl)pyrrolidin-2-one (**10**)*.[58] Yield: 20%. ^{1}H NMR (400 MHz, $CDCl_3$) δ: 7.92 (d, J = 15.6 Hz, 1H, Ar-CH=CH-), 7.75 (d, J = 15.6 Hz, 1H, Ar-CH=CH-), 7.52 (d, J = 8.8 Hz, 2H, ArH_2), 7.47 (d, J = 8.8 Hz, 2H, ArH_2), 3.92 (t, 2H, N-CH_2-), 2.66 (t, 2H, -$COCH_2$-), 2.09 (m, 2H, -CH_2-); ^{13}C NMR (100 MHz, $CDCl_3$) δ: 176.0, 166.3, 144.2, 134.0, 132.3, 130.1, 124.8, 119.9, 46.1, 34.2, 17.4; EI-MS m/z (%): 293 (M^+, 36), 211 (91), 209 (100), 183 (26), 102 (75), 84 (27); mp: 112-113 ^oC; purity: 99.23% (MeOH/H_2O = 65/35, R_t= 11.508 min).

*(E)-1-(3-(4-(Trifluoromethyl)phenyl)acryloyl)piperidin-2-one (**11**).* Yield: 40%. ^{1}H NMR (400 MHz, DMSO-d_6) δ: 7.84 (d, J = 8.0 Hz, 2H, ArH_2), 7.78 (d, J = 8.0 Hz, 2H, ArH_2), 7.56 (d, J = 15.6 Hz, 1H, Ar-CH=CH-), 7.41 (d, J = 15.6 Hz, 1H, Ar-CH=CH-), 3.68 (t, 2H, N-CH_2-), 2.53 (t, 2H, -$COCH_2$-), 1.80(m, 4H, -CH_2CH_2-); ^{13}C NMR (100 MHz, $CDCl_3$) δ: 174.2, 169.5, 141.1, 138.8, 131.8, 131.4, 128.6, 126.0, 125.9, 124.9, 122.8, 45.0, 35.2, 22.8, 20.9; ESI-MS (m/z): [M + H^+] 298.7; mp: 86-87 ^oC; purity: 99.68% (MeOH/H_2O = 65/35, R_t= 14.103 min).

*(E)-1-(3-(4-Nitrophenyl)acryloyl)piperidin-2-one (**12**).* Yield: 35%. ^{1}H NMR (400 MHz, DMSO-d_6) δ: 8.26 (d, J = 8.8 Hz, 2H, ArH_2), 7.89 (d, J = 8.8 Hz, 2H, ArH_2), 7.58 (d, J = 16.0 Hz, 1H, Ar-CH=CH-), 7.44 (d, J = 16.0 Hz, 1H, Ar-CH=CH-), 3.68 (t, 2H, N-CH_2-), 2.54 (t, 2H, -$COCH_2$-), 1.80 (m, 4H, -CH_2CH_2-); ^{13}C NMR (100 MHz, $CDCl_3$) δ: 174.2, 169.0, 148.3, 141.6, 139.4, 128.8, 126.5, 124.2, 44.9, 35.0, 22.6, 20.7; EI-MS m/z (%): 274 (M^+, 100), 246 (41), 176 (95), 130 (80), 102(34); mp: 146-148 ^oC; purity: 95.87% (MeOH/H_2O = 70/30, R_t= 4.579 min).

*(E)-1-(3-(4-Bromophenyl)acryloyl)piperidin-2-one (**13**).* Yield: 30%. ^{1}H NMR (400 MHz,

DMSO-d_6) δ: 7.94 (d, J = 16.0 Hz, 1H, Ar-CH=CH-), 7.83 (d, J = 16.0 Hz, 1H, Ar-CH=CH-), 7.61 (d, 2H, ArH_2), 7.38 (d, 2H, ArH_2), 3.92 (t, 2H, N-CH_2-), 2.65 (t, 2H, -$COCH_2$-), 2.06 (m, 4H, -CH_2CH_2-); ^{13}C NMR (100 MHz, $CDCl_3$) δ: 174.1, 169.6, 141.8, 134.2, 132.1, 129.8, 124.3, 122.9, 44.8, 35.1, 22.7, 20.8; ESI-MS (m/z): [M + Na^+] 330.0; mp: 114-116 ^oC; purity: 98.98% (MeOH/H_2O = 70/30, R_t= 8.771 min).

*(E)-1-(3-(4-(Trifluoromethyl)phenyl)acryloyl)azepan-2-one (**14**).* Yield: 25%. ^{1}H NMR (400 MHz, DMSO-d_6) δ: 7.85 (d, J = 8.4 Hz, 2H, ArH_2), 7.78 (d, J = 8.4 Hz, 2H, ArH_2), 7.55 (d, J=16.0, 1H, Ar-CH=CH-), 7.39 (d, J=16.0, 1H, Ar-CH=CH-), 3.92 (t, 2H, N-CH_2-), 2.76 (t, 2H, -$COCH_2$-), 1.72-1.62 (m, 6H, -$CH_2CH_2CH_2$-); ^{13}C NMR (100 MHz, $CDCl_3$) δ: 178.5, 168.7, 141.1, 138.8, 131.2, 128.5, 125.9, 125.9, 124.8, 44.0, 39.8, 29.5, 28.8, 23.9; ESI-MS (m/z): [M + H^+] 312.5; mp: 89-90 ^oC; purity: 99.75% (MeOH/H_2O = 70/30, R_t= 12.299 min).

*(E)-1-(3-(4-Nitrophenyl)acryloyl)azepan-2-one (**15**).* Yield: 25%. ^{1}H NMR (400 MHz, DMSO-d_6) δ: 8.26 (d, J = 8.8 Hz, 2H, ArH_2), 7.90 (d, J = 8.8 Hz, 1H, ArH_2), 7.57 (d, J=16.0, 1H, Ar-CH=CH-), 7.43 (d, J=16.0, 1H, Ar-CH=CH-), 3.93 (t, 2H, N-CH_2-), 2.76 (t, 2H, -$COCH_2$-), 1.72-1.65 (m, 6H, -$CH_2CH_2CH_2$-); ^{13}C NMR (100 MHz, $CDCl_3$) δ: 178.5, 168.4, 148.4, 141.6, 139.6, 129.6, 126.6, 124.3, 123.7, 44.1, 39.7, 29.4, 28.8, 23.9; EI-MS m/z (%): 288 (M^+, 100), 260 (15), 176 (56), 130 (47), 102 (20); mp: 82-84 ^oC; purity: 99.91% (MeOH/H_2O = 70/30, R_t= 6.102 min).

*1-Cinnamoylpyrrolidin-2-one (**16**).*[59] Yield: 43%. ^{1}H NMR (400 MHz, $CDCl_3$) δ: 7.94 (d, J = 16.0 Hz, 1H, Ar-CH=CH-), 7.83 (d, J = 16.0 Hz, 1H, Ar-CH=CH-), 7.61 (d, 2H, ArH_2), 7.38 (m, 3H, ArH_3), 3.92 (t, 2H, N-CH_2-), 2.65 (t, 2H, -$COCH_2$-), 2.06 (m, 2H, -CH_2-); ^{13}C NMR (100 MHz, $CDCl_3$) δ: 175.6, 166.2, 145.4, 134.8, 130.3, 128.7, 128.4, 118.9, 45. 8, 33.9, 17.1; ESI-MS (m/z):

[M + H^+] 215.8; mp: 98-99 ^oC; purity: 99.97% (MeOH/H_2O = 65/35, R_t= 5.687 min).

*1-Cinnamoylpiperidin-2-one (**17**)*.[59] Yield: 45%. ^1H NMR (400 MHz, $CDCl_3$) δ: 7.72 (d, J = 15.6 Hz, 1H, Ar-CH=CH-), 7.58 (d, 2H, ArH_2), 7.45 (d, J = 15.6 Hz, 1H, Ar-CH=CH-), 7.35 (m, 3H, ArH_3), 3.81 (t, 2H, N-CH_2-), 2.62 (t, 2H, -$COCH_2$-), 1.90 (m, 4H, -CH_2CH_2-); ^{13}C NMR (100 MHz, $CDCl_3$) δ: 173.8, 169.6, 143.0, 135.0, 129. 9, 128.7, 128.2, 122.0, 44.5, 34.8, 22.4, 20.6; ESI-MS (m/z): [M + H^+] 229.9; mp: 57-58 ^oC; purity: 96.56% (MeOH/H_2O = 65/35, R_t= 6.629 min).

*1-Cinnamoylazepan-2-one (**18**).* Yield: 37%. ^1H NMR (400 MHz, $CDCl_3$) δ: 7.70 (d, J = 16.0 Hz, 1H, Ar-CH=CH-), 7.57 (d, 2H, ArH_2), 7.40 (d, J = 16.0 Hz, 1H, Ar-CH=CH-), 7.36 (m, 3H, ArH_3), 3.97 (m, 2H, N-CH_2-), 2.77 (m,, 2H, -$COCH_2$-), 1.81 (m, 6H, -$CH_2CH_2CH_2$-); ^{13}C NMR (100 MHz, $CDCl_3$) δ: 178.2, 169.0, 143.2, 135.2, 130.0, 128.8, 128.3, 122.1, 43.8, 39.6, 29.3, 28.7, 23.8; ESI-MS (m/z): [M + Na^+] 266.0; mp: 70-71 ^oC; purity: 99.17% (MeOH/H_2O = 65/35, R_t= 9.557 min).

*(E)-4-(3-oxo-3-(2-oxopyrrolidin-1-yl)prop-1-en-1-yl)phenyl acetate(**19a**)*. Yield: **56%**; ^1H NMR (400 MHz, $CDCl_3$) δ: 7.90 (d, J = 15.6 Hz, 1H, Ar-CH=CH-), 7.80 (d, J = 15.6 Hz, 1H, Ar-CH=CH-), 7.64 (d, J = 8.4 Hz, 2H, ArH_2), 7.12 (d, J = 8.4 Hz, 2H, ArH_2), 3.91 (t, 2H, N-CH_2-), 2.65 (t, 2H, -$COCH_2$-), 2.31 (s, 3H, -$COCH_3$), 2.07 (m, 2H, -CH_2-); ^{13}C NMR (100 MHz, $CDCl_3$) δ: 175.8, 169.2, 166.2, 152.2, 144.4, 132.7, 129.7, 122.1, 119.3, 45.9, 34.0, 21.2, 17.3; ESI-MS (m/z): [M + H^+] 274.8; mp: 154-155 ^oC.

*Synthesis of **B8** (Step e in Scheme 1).* To a solution of *p*-coumaric acid (**B8a**, 10 mmol, 1.64g) in 4 mL acetic anhydride was added DMAP (0.08 equiv.) and catalytic amount of pyridine (0.01 equiv.). The mixture was heated to reflux for 4 h before it was washed with saturated aqueous $NaHCO_3$, and extracted with ethyl acetate. The combined organic phases were dried over $MgSO_4$.

After filtration and concentration, the residue was purified by flash chromatography to obtain the desired product. Yield: 92%.

*Synthesis of **19** (Step f in Scheme 1). T*o a solution of amide (0.37 mmol, 100 mg) in dry CH_2Cl_2 (10 mL) was added pyrollidine (1 mL). The reaction mixture was stirred for 15 min at room temperature. The reaction was quenched with HCl (20 mL, 1 M) and extracted with ethyl acetate. The combined organic phases were dried over $MgSO_4$. After filtration and concentration, the residue was purified by flash chromatography to obtain the desired product.

*(E)-1-(3-(4-hydroxyphenyl)acryloyl)pyrrolidin-2-one(**19**)*.[59] Yield: 66%; ^{1}H NMR (400 MHz, DMSO-d_6) δ: 10.04(s, 1H, Ar-OH), 7.69(d, J = 16.0 Hz, 1H, Ar-CH=CH-), 7.64(d, J = 16.0 Hz, 1H, Ar-CH=CH-), 7.49(d, J = 7.2 Hz, 2H, ArH_2), 7.64(d, J = 7.2 Hz, 2H, ArH_2), 3.76(t, J = 7.2 Hz, 2H, N-CH_2-), 2.57(t, J = 8.2 Hz, 2H, -$COCH_2$-), 1.96(m, 2H, -CH_2-); ^{13}C NMR (100 MHz, DMSO-d_6) δ: 175.8, 165.5, 159.9, 144.3, 130.1, 125.6, 115.9, 115. 6, 45.5, 33.4, 16.6; mp: 201-202 ^{o}C; ESI-MS (m/z): [M + H^+] 232.0. purity: 96.58% (MeOH/H_2O = 48/52, R_t = 6.773 min).

Biological Studies. *Cell cultures.* PC12 cells (rat adrenal pheochromocytoma cell line) and L02 cells (the normal liver cell line) were obtained from Shanghai Institute of Biochemistry and Cell Biology, Chinese Academy of Sciences and were cultured in DMEM supplemented with 10% FBS, 2 mM glutamine, and 100 units ml^{-1} penicillin/streptomycin and maintained in a humidified atmosphere of 5% CO_2 at 37 °C.

MTT assay and Lactate dehydrogenase (LDH) release assay. PC12 cells (1×10^4 cells/well) were seeded in 96-well plates for 1 day followed by incubation with the drugs for 24 h. The cytotoxicity of drugs was determined by the MTT assay according to our published procedure.[32, 33] For the H_2O_2 or 6-OHDA injury model, PC12 cells (1×10^4 cells/well) were plated in a 96-well plate

and allowed to adhere for 1 day, and then treated with the drugs for 24 h. After replacing with fresh medium containing 500 μM H_2O_2 or 200 μM 6-OHDA for 12 h, the cell viability was determined by the MTT assay. For the LDH release assay, the cells (2×10^5 cells/well) were plated in 12-well plates. On the following day, the cells were exposed to various concentrations of **4** or **5** for 24 h, followed by addition of 500 μM H_2O_2 or 200 μM 6-OHDA for 12 h. The leakage of LDH from the cultured cells was quantified by measuring LDH activity in the culture medium according to our published procedure.[13, 14]

Hoechst 33342 staining. PC12 cells (2×10^5 cells/well) were seeded into 12-well plates. On the following day, the cells were treated with **4** or **5** for another 24 h followed by replacing with the fresh medium containing 500 μM H_2O_2 or 200 μM 6-OHDA for 5 h. Hoechst 33342 was subsequently added to a final concentration of 5 μg/mL to stain the nuclei. The cells were visualized and photographed under a Leica inverted fluorescent microscopy. Cells displayed condensed and highly fluorescent nuclei, a characteristic morphology of cells undergoing apoptosis, were counted as apoptotic cells.

Measurement of caspase-3 activity. For determination of the caspase-3 activity, PC12 cells (1×10^6 cells/well) were seeded in 60-mm dishes for 24 h, and then treated with different concentrations of **4** or **5** for another 24 h. After replacing with the fresh medium containing 500 μM H_2O_2 or 200 μM 6-OHDA and continuing culture for 24 h, the cells were lysed with RIPA buffer (2 mM EDTA, 0.5% deoxycholate, 150 mM NaCl, 1% TritonX-100, 0.1% SDS, 1 mM Na_3VO_4, and 1 mM PMSF in 50 mM Tris–HCl, pH 7.5). The protein content was quantified by the Bradford procedure using BSA as a standard. The caspase-3 activity in the lysate was determined by a colorimetric assay using Ac-DEVD-pNA as a substrate.[30, 31] The activity of caspase-3 in the

drug-treated cells was expressed as the percentage of the control cells.

Determination of intracellular ROS.[32, 33] For assaying the intracellular accumulation of ROS, PC12 cells (2×10^5cells/well) were seeded into 12-well plates. After 24 h, the cells were treated with **4** or **5** for another 24 h followed by replacing with the fresh medium containing 500 μM H_2O_2 or 200 μM 6-OHDA for 5 h. After removing the medium, DCFH-DA (10 μM) in fresh FBS-free medium was added, and continued incubation for 30 min at 37 °C in dark. The cells were visualized and photographed under fluorescent microscopy. The appearance of green fluorescence indicates the accumulation of ROS in cells.

Assessment of intracellular thiols. PC12 cells were plated in 60-mm dishes at a concentration of 8×10^5 cells/well and allowed to adhere for 24 h, then were treated with **4** or **5** (0-20 μM) for 24 h followed treated with H_2O_2 or 6-OHDA for another 24 h in the absence of drugs. The cells were collected, washed twice with PBS, and lysed with RIPA buffer for 30 min on ice. The protein content was quantified by the Bradford procedure using BSA as a standard. Total thiol levels were determined by DTNB-titration.[31-33, 60] Briefly, 10 μL of cell lysate was added to cuvettes containing 90 μL of 1 mM DTNB in 6 M guanidine hydrochloride, pH 8.0. After keeping the mixture for 5 min at room temperature, the absorbance was read at 412 nm. Thiol levels were calculated by a calibration curve using GSH as the standard.

Real-time reverse transcription-PCR (RT-PCR). PC12 cells (1×10^6 cells/well) were seeded in 60-mm dishes for 1 day, and treated with **4** or **5** (20 μM) for 0, 3, 6 and 12 h. Total RNA was isolated from cells using the RNAiso plus (TaKaRa, Dalian, China) according to the manufacture's protocol and quantified through 260/280 absorbance. Reverse transcription was performed using Primescript™ RT reagent kit according to the manufacture's protocol (TaKaRa, Dalian, China).

RT-PCR was performed on Mx3005PRT-PCR System (Agilent Technologies) using Power SYBR Green PCR Master Mix. The glyceraldehyde-3-phosphate dehydrogenase (GAPDH) was used as an internal control. Target gene expression was measured and normalized to the GAPDH expression level. PCR primers specific to each gene are as follows: GAPDH: 5'-cagtgccagcctcgtctcat-3' and 5'-aggggccatccacagtcttc-3'; HO-1: 5'-gccctggaagaggagatagag-3' and 5'-tagtgctgtgtggctggtgt-3'; NQO1: 5'-tcaccactctactttgctccaa-3' and 5'-ttttctgctcctcttgaacctc-3'; Trx1: 5'-ccttctttcattccctctgtgac-3' and 5'-cccaacctttgaccctttttat-3'; TrxR1: 5'-actgctcaatccacaaacagc-3' and 5'-ccacggtctctaagccaatagt-3'; glutamate cysteine ligase catalytic subunit (GCLC): 5'-caaggacaagaacacaccatct-3' and 5'-cagcactcaaagccataacaat-3'; glutamate cysteine ligase modifier subunit (GCLM): 5'-ggcacaggtaaaacccaatagt-3' and 5'-ttcaatgtcagggatgctttct-3'. The GAPDH was used as an internal control.

Measurement of total glutathione. After the drug treatment, the cells were collected and resuspended in extraction buffer containing 0.1% TritonX-100 and 0.6% sulfosalicyclic acid in 0.1 M PBS with 5 mM EDTA, pH 7.5 (KPE buffer). The suspension was sonicated on ice for 2-3 min with vortexing every 30 s. After centrifugation at 3000 g for 4 min at 4 °C, the supernatant was ready for the total GSH assay by enzymatic detection as described in the published protocols.[33, 61]

Determination of NQO1 activity. For measuring NQO1, the cells were lysed in RIPA buffer. The total protein content was quantified by the Bradford procedure using BSA as a standard. The NQO1 activity was determined spectrophotometrically by monitoring the reduction of the electron acceptor DCPIP at 600 nm.[13, 14, 62] The enzymatic reaction was initiated by the addition of cell lysate (5 μg of total protein) to the reaction mixture (20 mM Tris-HCl, pH 7.4, 200 μM NADH, and 40 μM DCPIP), and the decrease in absorbance at 600 nm was measured every 8 s for 2 min at room

temperature in the presence or absence of 20 μM dicoumarol, a specific inhibitor of NQO1. The dicoumarol-inhibitable part of DCPIP's reduction was used to calculate the NQO1 activity. The same amounts of DMSO were added to the control experiments and the activity was expressed as the percentage of the control.

Trx and TrxR activity assays. Measuring cellular Trx and TrxR activity were performed by following our published protocols.[30, 31, 63] Briefly, the cell extract containing 20 μg of total proteins was incubated in a final reaction volume of 50 μL 100 mM Tris-HCl (pH 7.4) containing 0.3 mM insulin, 660 μM NADPH, 3 mM EDTA and 60 nM recombinant rat TrxR1 (for assaying the Trx activity) or 4 μM E. coli Trx (for assaying the TrxR activity) for 30 min at 37 °C. The reaction was terminated by adding 200 μL of 1 mM DTNB in 6 M guanidine hydrochloride, pH 8.0. A blank sample, containing everything except Trx (for TrxR assay) or TrxR (for Trx assay), was treated in the same manner. The absorbance at 412 nm was measured, and the blank value was subtracted from the corresponding absorbance value of the sample. The same amounts of DMSO were added to the control experiments and the activity was expressed as the percentage of the control.

Determination of TrxR activity by TRFS-green. TRFS-green, developed by our group, is a cell membrane permeable dye, which specifically detects the activity of TrxR in the cultured cells.[34] PC12 cells (2×10^5 cells/well) were seeded into 12-well plates. After 24 h, the cells were treated with **4** or **5** for 20 h. Then TRFS-green was added (the final concentration is 10 μM) and continued incubation for 4 h at 37 °C in dark. The cells were visualized and photographed under fluorescent microscopy. The intensity of the green fluorescence indicates the relative activity of TrxR in cells.

Preparation of different protein extracts for Western blots analysis. Different protein extracts from PC12 cells, i. e., the whole cell protein extract, the cytosolic protein extract and the nuclear

protein extract, were prepared according to our previously published procedures.[13, 14] The target proteins were determined by Western blots.

Knockdown of Nrf2 expression by shRNA transfection. The shRNA (shNrf2-842) targeting rat Nrf2 gene was used for Nrf2 knockdown experiments.[13, 14] The shRNA with scrambled sequence (shNT) was used as a control. Exponentially growing cells were transfected with different shRNAs using GeneTran III transfection reagent according to the manufacture's instruction. After 48 h of transfection, the cells were maintained in DMEM containing 10% FBS, 2 mM glutamine, 100 units/ml penicillin/streptomycin at 37℃ in a humidified atmosphere of 5% CO_2 and selected by supplementation with 0.5 mg/ml of G418. Knockdown of the Nrf2 expression in the cells was analyzed by Western blotting.

Determination of cLogP and PSA. The cLogP values were obtained by determining their partition coefficients between *n*-octanol and water according to the published procedure and *o*-cresol was used as a positive control.[36, 64] The octanol–water partition coefficient was determined as the follows. Approximately 100 mL of *n*-octanol and 100 ml of distilled water were thoroughly mixed in a 500 mL separatory funnel to get mutually saturated. To an Erlenmeyer flask containing approximately 5 mg of tested compound in 10 ml of water-saturated octanol was added the same volume of octanol-saturated water. The flask was then shaked for 3 h at 25 ^{o}C to reach the equilibrium. The two phases were separated by a separating funnel. Aliquots of water phase (100 μL) and octanol phase (100 μL) were transferred to cuvettes containing 1900 μL of methanol, and the concentrations of the compound in octanol phase (C1) and in water phase (C2) were quantified by measuring the absorbance at 315 nm from an established calibration curve of the compound. The cLogP value was calculated by the equation: cLogP=log(C1/C2). The PSA values were calculated

on line via the website: www.molinspiration.com.

Statistics. Data are presented as mean ± S. E. Statistical differences between two groups were assessed by the Students *t*-test. Comparisons among multiple groups were performed using one-way analysis of variance (ANOVA), followed by a post hoc Scheffe test. $P<0.05$ was used as the criterion for statistical significance.

SUPPORTING INFORMATION

Supporting Information Available: The details of the synthetic intermediates, in vitro free radical scavenging assay, HPLC chromatograms and NMR spectra of the final compounds. This material is available free of charge via the Internet at http://pubs.acs.org.

AUTHOR INFORMATION

Corresponding Author

E-mail: fangjg@lzu.edu.cn. Phone: +86 931-8912500.

Author Contributions

[#] These authors contribute equally to this work.

ACKNOWLEDGMENTS

The financial supports from Lanzhou University (the Fundamental Research Funds for the Central Universities, lzujbky-2014-56) and Natural Science Foundation of Gansu Province (145RJZA225) are greatly acknowledged. The authors also express appreciation to Prof. Kun Gao at the SKLAOC

and her group members for assistance of HPLC analysis, and to Prof. Arne Holmgren at Karolinska Institute for the recombinant rat TrxR1. The authors confirm that there are no conflicts of interest.

ABBREVATIONS USED

AAPH: 2,2'-azobis(2-methylpropionamidine) dihydrochloride; ABTS: 2,2′-azinobis-(3-ethylbenzothiazoline-6-sulfonic acid); ARE: antioxidant response elements; BBB: blood-brain barrier; DCFH-DA: 2',7'-dichlorofluorescin diacetate; DCPIP: 2,6-dichlorophenol-indophenol; DPPH: 2,2-diphenyl-1-picrylhydrazyl; DTNB: 5,5'-dithiobis-2-nitrobenzoic acid; GAPDH: glyceraldehyde-3-phosphate dehydrogenase; GCLC: glutamate cysteine ligase catalytic subunit; GCLM: glutamate cysteine ligase modifier subunit; GR: glutathione reductase; GSH: reduced glutathione; HO-1: heme oxygenase-1 (HO-1); Keap1: Kelch-like ECH-associated protein 1; LDH: lactate dehydrogenase; MTT: 3-(4,5-dimethyl-2-thiazolyl)-2,5-diphenyl-2-H-tetrazolium bromide; NQO1: NAD(P)H quinone oxidoreductase 1; Nrf2: nuclear factor erythroid 2-related factor 2; 6-OHDA: 6-hydroxydopamine; PL: piperlongumine; PC12-shNrf2: PC12 cells stably transfected with shRNA specifically targeting Nrf2; PC12-shNT: PC12 cells stably transfected with non-targeting shRNA; ROS: reactive oxygen species; SAR: structure-activity relationship; TRFS-green: thioredoxin reductase fluorogenic substrate; Trx1: thioredoxin 1; TrxR 1: thioredoxin reductase 1.

REFERENCES

1. Ray, P. D.; Huang, B. W.; Tsuji, Y. Reactive oxygen species (ROS) homeostasis and redox regulation in cellular signaling. *Cell Signal* **2012,** 24, 981-90.
2. Sauer, H.; Wartenberg, M.; Hescheler, J. Reactive oxygen species as intracellular messengers during cell growth and differentiation. *Cell Physiol Biochem* **2001,** 11, 173-86.
3. Bindoli, A.; Rigobello, M. P. Principles in redox signaling: from chemistry to functional significance. *Antioxid Redox Signal* **2013,** 18, 1557-93.
4. Barnham, K. J.; Masters, C. L.; Bush, A. I. Neurodegenerative diseases and oxidative stress. *Nat Rev Drug Discov* **2004,** 3, 205-14.
5. Lin, M. T.; Beal, M. F. Mitochondrial dysfunction and oxidative stress in neurodegenerative diseases. *Nature* **2006,** 443, 787-95.
6. Trippier, P. C.; Jansen Labby, K.; Hawker, D. D.; Mataka, J. J.; Silverman, R. B. Target- and mechanism-based therapeutics for neurodegenerative diseases: strength in numbers. *J Med Chem* **2013,** 56, 3121-47.
7. Uttara, B.; Singh, A. V.; Zamboni, P.; Mahajan, R. T. Oxidative stress and neurodegenerative diseases: a review of upstream and downstream antioxidant therapeutic options. *Curr Neuropharmacol* **2009,** 7, 65-74.
8. Suzuki, T.; Motohashi, H.; Yamamoto, M. Toward clinical application of the Keap1-Nrf2 pathway. *Trends Pharmacol Sci* **2013,** 34, 340-6.
9. Ma, Q. Role of nrf2 in oxidative stress and toxicity. *Annu Rev Pharmacol Toxicol* **2013,** 53, 401-26.
10. Kobayashi, A.; Kang, M. I.; Okawa, H.; Ohtsuji, M.; Zenke, Y.; Chiba, T.; Igarashi, K.; Yamamoto, M. Oxidative stress sensor Keap1 functions as an adaptor for Cul3-based E3 ligase to regulate proteasomal degradation of Nrf2. *Mol Cell Biol* **2004,** 24, 7130-9.
11. Zhang, M.; An, C.; Gao, Y.; Leak, R. K.; Chen, J.; Zhang, F. Emerging roles of Nrf2 and phase II antioxidant enzymes in neuroprotection. *Prog Neurobiol* **2013,** 100, 30-47.
12. Calkins, M. J.; Johnson, D. A.; Townsend, J. A.; Vargas, M. R.; Dowell, J. A.; Williamson, T. P.; Kraft, A. D.; Lee, J. M.; Li, J.; Johnson, J. A. The Nrf2/ARE pathway as a potential therapeutic target in neurodegenerative disease. *Antioxid Redox Signal* **2009,** 11, 497-508.
13. Yao, J.; Zhang, B.; Ge, C.; Peng, S.; Fang, J. Xanthohumol, a Polyphenol Chalcone Present in Hops, Activating Nrf2 Enzymes To Confer Protection against Oxidative Damage in PC12 Cells. *J Agric Food Chem* **2015,** 63, 1521-31.
14. Yao, J.; Ge, C.; Duan, D.; Zhang, B.; Cui, X.; Peng, S.; Liu, Y.; Fang, J. Activation of the Phase II Enzymes for Neuroprotection by Ginger Active Constituent 6-Dehydrogingerdione in PC12 Cells. *J Agric Food Chem* **2014,** 62, 5507-5518.
15. Magesh, S.; Chen, Y.; Hu, L. Small molecule modulators of Keap1-Nrf2-ARE pathway as potential preventive and therapeutic agents. *Med Res Rev* **2012,** 32, 687-726.
16. Hur, W.; Gray, N. S. Small molecule modulators of antioxidant response pathway. *Curr Opin Chem Biol* **2011,** 15, 162-73.
17. Bezerra, D. P.; Pessoa, C.; de Moraes, M. O.; Saker-Neto, N.; Silveira, E. R.; Costa-Lotufo, L. V. Overview of the therapeutic potential of piplartine (piperlongumine). *Eur J Pharm Sci* **2013,** 48, 453-63.
18. Iwashita, M.; Oka, N.; Ohkubo, S.; Saito, M.; Nakahata, N. Piperlongumine, a constituent of Piper longum L., inhibits rabbit platelet aggregation as a thromboxane A(2) receptor antagonist. *Eur J Pharmacol* **2007,** 570, 38-42.
19. Rodrigues Silva, D.; Baroni, S.; Svidzinski, A. E.; Bersani-Amado, C. A.; Cortez, D. A. Anti-inflammatory activity of the extract, fractions and amides from the leaves of Piper ovatum Vahl (Piperaceae). *J Ethnopharmacol* **2008,** 116, 569-73.
20. Son, D. J.; Kim, S. Y.; Han, S. S.; Kim, C. W.; Kumar, S.; Park, B. S.; Lee, S. E.; Yun, Y. P.; Jo, H.; Park, Y. H.

Piperlongumine inhibits atherosclerotic plaque formation and vascular smooth muscle cell proliferation by suppressing PDGF receptor signaling. *Biochem Biophys Res Commun* **2012,** 427, 349-54.

21. Raj, L.; Ide, T.; Gurkar, A. U.; Foley, M.; Schenone, M.; Li, X.; Tolliday, N. J.; Golub, T. R.; Carr, S. A.; Shamji, A. F.; Stern, A. M.; Mandinova, A.; Schreiber, S. L.; Lee, S. W. Selective killing of cancer cells by a small molecule targeting the stress response to ROS. *Nature* **2011,** 475, 231-4.

22. Wu, Y.; Min, X.; Zhuang, C.; Li, J.; Yu, Z.; Dong, G.; Yao, J.; Wang, S.; Liu, Y.; Wu, S.; Zhu, S.; Sheng, C.; Wei, Y.; Zhang, H.; Zhang, W.; Miao, Z. Design, synthesis and biological activity of piperlongumine derivatives as selective anticancer agents. *Eur J Med Chem* **2014,** 82, 545-51.

23. Seo, Y. H.; Kim, J. K.; Jun, J. G. Synthesis and biological evaluation of piperlongumine derivatives as potent anti-inflammatory agents. *Bioorg Med Chem Lett* **2014,** 24, 5727-30.

24. Boskovic, Z. V.; Hussain, M. M.; Adams, D. J.; Dai, M.; Schreiber, S. L. Synthesis of piperlogs and analysis of their effects on cells. *Tetrahedron* **2013,** 69, 7559-7567.

25. Adams, D. J.; Dai, M.; Pellegrino, G.; Wagner, B. K.; Stern, A. M.; Shamji, A. F.; Schreiber, S. L. Synthesis, cellular evaluation, and mechanism of action of piperlongumine analogs. *Proc Natl Acad Sci U S A* **2012,** 109, 15115-20.

26. Barcelos, R. C.; Pelizzaro-Rocha, K. J.; Pastre, J. C.; Dias, M. P.; Ferreira-Halder, C. V.; Pilli, R. A. A new goniothalamin N-acylated aza-derivative strongly downregulates mediators of signaling transduction associated with pancreatic cancer aggressiveness. *Eur J Med Chem* **2014,** 87, 745-58.

27. Yang, S. X.; Kang, T. N.; Rui, C. H.; Yang, X. L.; Sun, Y. F.; Cui, Z. N.; Lin, Y. Design, Synthesis, and Insecticidal Activity of 1,5-Diphenyl-1-pentanone Analogues. *Chin J Chem* **2011,** 29, 2394-2400.

28. Ning, X.; Guo, Y.; Wang, X.; Ma, X.; Tian, C.; Shi, X.; Zhu, R.; Cheng, C.; Du, Y.; Ma, Z.; Zhang, Z.; Liu, J. Design, synthesis, and biological evaluation of (e)-3,4-dihydroxystyryl aralkyl sulfones and sulfoxides as novel multifunctional neuroprotective agents. *J Med Chem* **2014,** 57, 4302-12.

29. Saito, Y.; Nishio, K.; Ogawa, Y.; Kinumi, T.; Yoshida, Y.; Masuo, Y.; Niki, E. Molecular mechanisms of 6-hydroxydopamine-induced cytotoxicity in PC12 cells: involvement of hydrogen peroxide-dependent and -independent action. *Free Radic Biol Med* **2007,** 42, 675-85.

30. Zhang, B.; Duan, D.; Ge, C.; Yao, J.; Liu, Y.; Li, X.; Fang, J. Synthesis of xanthohumol analogues and discovery of potent thioredoxin reductase inhibitor as potential anticancer agent. *J Med Chem* **2015,** 58, 1795-805.

31. Liu, Y.; Duan, D.; Yao, J.; Zhang, B.; Peng, S.; Ma, H.; Song, Y.; Fang, J. Dithiaarsanes Induce Oxidative Stress-Mediated Apoptosis in HL-60 Cells by Selectively Targeting Thioredoxin Reductase. *J Med Chem* **2014,** 57, 5203-11.

32. Duan, D.; Zhang, B.; Yao, J.; Liu, Y.; Sun, J.; Ge, C.; Peng, S.; Fang, J. Gambogic acid induces apoptosis in hepatocellular carcinoma SMMC-7721 cells by targeting cytosolic thioredoxin reductase. *Free Radic Biol Med* **2014,** 69, 15-25.

33. Duan, D.; Zhang, B.; Yao, J.; Liu, Y.; Fang, J. Shikonin targets cytosolic thioredoxin reductase to induce ROS-mediated apoptosis in human promyelocytic leukemia HL-60 cells. *Free Radic Biol Med* **2014,** 70, 182-93.

34. Zhang, L.; Duan, D.; Liu, Y.; Ge, C.; Cui, X.; Sun, J.; Fang, J. Highly selective off-on fluorescent probe for imaging thioredoxin reductase in living cells. *J Am Chem Soc* **2014,** 136, 226-33.

35. Pajouhesh, H.; Lenz, G. R. Medicinal chemical properties of successful central nervous system drugs. *NeuroRx* **2005,** 2, 541-53.

36. Sangster, J. Octanol-Water Partition Coefficients of Simple Organic Compounds. *J Phys Chem Ref Data* **1989,** 18, 1111-1227.

37. Murphy, M. P. How mitochondria produce reactive oxygen species. *Biochem J* **2009,** 417, 1-13.

38. Sena, L. A.; Chandel, N. S. Physiological roles of mitochondrial reactive oxygen species. *Mol Cell* **2012,** 48,

158-67.

39. Trachootham, D.; Alexandre, J.; Huang, P. Targeting cancer cells by ROS-mediated mechanisms: a radical therapeutic approach? *Nat Rev Drug Discov* **2009,** 8, 579-91.

40. Klein, J. A.; Ackerman, S. L. Oxidative stress, cell cycle, and neurodegeneration. *J Clin Invest* **2003,** 111, 785-93.

41. Barone, M. C.; Sykiotis, G. P.; Bohmann, D. Genetic activation of Nrf2 signaling is sufficient to ameliorate neurodegenerative phenotypes in a Drosophila model of Parkinson's disease. *Dis Model Mech* **2011,** 4, 701-7.

42. Xiong, X. X.; Liu, J. M.; Qiu, X. Y.; Pan, F.; Yu, S. B.; Chen, X. Q. Piperlongumine induces apoptotic and autophagic death of the primary myeloid leukemia cells from patients via activation of ROS-p38/JNK pathways. *Acta Pharmacol Sin* **2015,** 36, 362-74.

43. Satoh, T.; McKercher, S. R.; Lipton, S. A. Nrf2/ARE-mediated antioxidant actions of pro-electrophilic drugs. *Free Radic Biol Med* **2013,** 65C, 645-657.

44. Zhang, B.; Ge, C.; Yao, J.; Liu, Y.; Xie, H.; Fang, J. Selective selenol fluorescent probes: design, synthesis, structural determinants, and biological applications. *J Am Chem Soc* **2015,** 137, 757-69.

45. Zhang, L. W.; Duan, D. Z.; Cui, X. M.; Sun, J. Y.; Fang, J. G. A selective and sensitive fluorescence probe for imaging endogenous zinc in living cells. *Tetrahedron* **2013,** 69, 15-21.

46. Cai, W.; Zhang, B.; Duan, D.; Wu, J.; Fang, J. Curcumin targeting the thioredoxin system elevates oxidative stress in HeLa cells. *Toxicol Appl Pharmacol* **2012,** 262, 341-8.

47. Cai, W. Q.; Zhang, L. W.; Song, Y. L.; Wang, B. L.; Zhang, B. X.; Cui, X. M.; Hu, G. M.; Liu, Y. P.; Wu, J. C.; Fang, J. G. Small molecule inhibitors of mammalian thioredoxin reductase. *Free Radical Biology and Medicine* **2012,** 52, 257-265.

48. Liu, H.; Luo, R.; Chen, X.; Liu, J.; Bi, Y.; Zheng, L.; Wu, X. Tissue distribution profiles of three antiparkinsonian alkaloids from Piper longum L. in rats determined by liquid chromatography-tandem mass spectrometry. *J Chromatogr B Analyt Technol Biomed Life Sci* **2013,** 928, 78-82.

49. Wilson, A. J.; Kerns, J. K.; Callahan, J. F.; Moody, C. J. Keap calm, and carry on covalently. *J Med Chem* **2013,** 56, 7463-76.

50. Kumar, V.; Kumar, S.; Hassan, M.; Wu, H.; Thimmulappa, R. K.; Kumar, A.; Sharma, S. K.; Parmar, V. S.; Biswal, S.; Malhotra, S. V. Novel chalcone derivatives as potent Nrf2 activators in mice and human lung epithelial cells. *J Med Chem* **2011,** 54, 4147-59.

51. Phillips, J. T.; Fox, R. J. BG-12 in multiple sclerosis. *Semin Neurol* **2013,** 33, 56-65.

52. Takaya, J.; Tadami, S.; Ukai, K.; Iwasawa, N. Copper(I)-catalyzed carboxylation of aryl- and alkenylboronic esters. *Org Lett* **2008,** 10, 2697-700.

53. Haadsma-Svensson, S. R.; Cleek, K. A.; Dinh, D. M.; Duncan, J. N.; Haber, C. L.; Huff, R. M.; Lajiness, M. E.; Nichols, N. F.; Smith, M. W.; Svensson, K. A.; Zaya, M. J.; Carlsson, A.; Lin, C. H. Dopamine D(3) receptor antagonists. 1. Synthesis and structure-activity relationships of 5,6-dimethoxy-N-alkyl- and N-alkylaryl-substituted 2-aminoindans. *J Med Chem* **2001,** 44, 4716-32.

54. Reddy, G. V.; Jacobs, H. K.; Gopalan, A. S.; Barrans, R. E., Jr.; Dietz, M. L.; Stepinski, D. C.; Herlinger, A. W. Synthesis of Symmetrical Methylenebis(Alkyl Hydrogen Phosphonates) by Selective Cleavage of Methylenebis(Dialkyl Phosphonates) with Morpholine. *Synth Commun* **2004,** 34, 331-344.

55. Rao, V. R.; Muthenna, P.; Shankaraiah, G.; Akileshwari, C.; Babu, K. H.; Suresh, G.; Babu, K. S.; Chandra Kumar, R. S.; Prasad, K. R.; Yadav, P. A.; Petrash, J. M.; Reddy, G. B.; Rao, J. M. Synthesis and biological evaluation of new piplartine analogues as potent aldose reductase inhibitors (ARIs). *Eur J Med Chem* **2012,** 57, 344-61.

56. Wang, Y. J.; Mao, J. W.; Wen, P. A mild highly effiient and green protocol for preparation of N-alk-2'-enoyl cyclic imides using basic ionic liquid [bmIm]OH as base and reaction medium. *J Chem Res* **2008**, 559–561.

57. Li, C. Y.; Tsai, W. J.; Damu, A. G.; Lee, E. J.; Wu, T. S.; Dung, N. X.; Thang, T. D.; Thanh, L. Isolation and

identification of antiplatelet aggregatory principles from the leaves of Piper lolot. *J Agric Food Chem* **2007,** 55, 9436-42.

58. Pineschi, M.; Del Moro, F.; Di Bussolo, V.; Macchia, F. Highly Enantioselective Copper-Phosphoramidite-Catalyzed Conjugate Addition of Dialkylzinc Reagents to Acyclic alpha, beta-Unsaturated Imides. *Adv. Synth. Catal.* **2006,** 348, 301-304.

59. Hoashi, Y.; Okino, T.; Takemoto, Y. Enantioselective Michael addition to alpha,beta-unsaturated imides catalyzed by a bifunctional organocatalyst. *Angew Chem Int Ed Engl* **2005,** 44, 4032-5.

60. Ellman, G. L. Tissue sulfhydryl groups. *Arch Biochem Biophys* **1959,** 82, 70-7.

61. Rahman, I.; Kode, A.; Biswas, S. K. Assay for quantitative determination of glutathione and glutathione disulfide levels using enzymatic recycling method. *Nat Protoc* **2006,** 1, 3159-65.

62. Benson, A. M.; Hunkeler, M. J.; Talalay, P. Increase of NAD(P)H:quinone reductase by dietary antioxidants: possible role in protection against carcinogenesis and toxicity. *Proc Natl Acad Sci U S A* **1980,** 77, 5216-20.

63. Fang, J.; Holmgren, A. Inhibition of thioredoxin and thioredoxin reductase by 4-hydroxy-2-nonenal in vitro and in vivo. *J Am Chem Soc* **2006,** 128, 1879-85.

64. Peng, S.; Zhang, B.; Yao, J.; Duan, D.; Fang, J. Dual protection of hydroxytyrosol, an olive oil polyphenol, against oxidative damage in PC12 cells *Food Funct.* **2015**. DOI: 10.1039/C5FO00097A.

Scheme, Table, Figures and Figure Legends

Scheme 1. Synthesis of PL and its analogues [a]

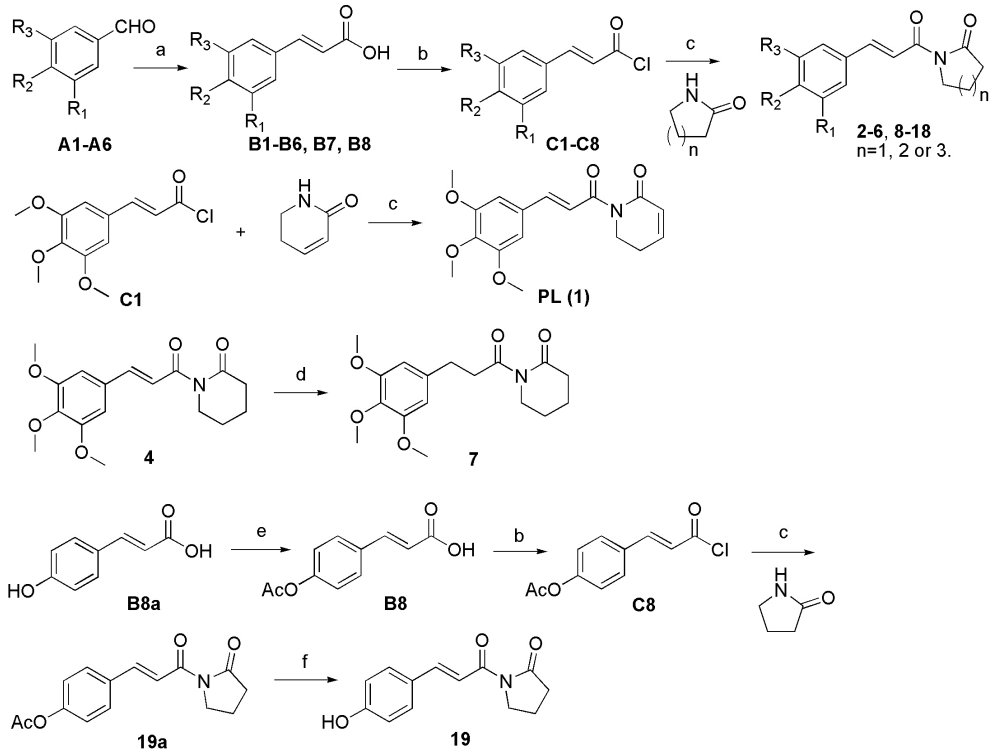

[a] Reaction condition: (a) Malonic acid, C_5H_5N, piperidine, reflux; (b) $(COCl)_2$, DMF, DCM, r.t.; (c) TEA, DCM, r.t.; (d) H_2, Pd/C, methanol; (e) Ac_2O, pyridine, DMAP, reflux; (f) pyrolidine, DCM, r.t.

Table 1 Medicinal chemical properties of **4** & **5**.

Compound #	cLogP [a]	PSA (Å^2) [b]	M. W.
4	1.88	65.08	319
5	1.79	46.61	245
CNS drug criteria	0-5	<70	<450

[a] The data was determined experimentally. [b] The data was calculated on line from the website: www.molinspiration.com.

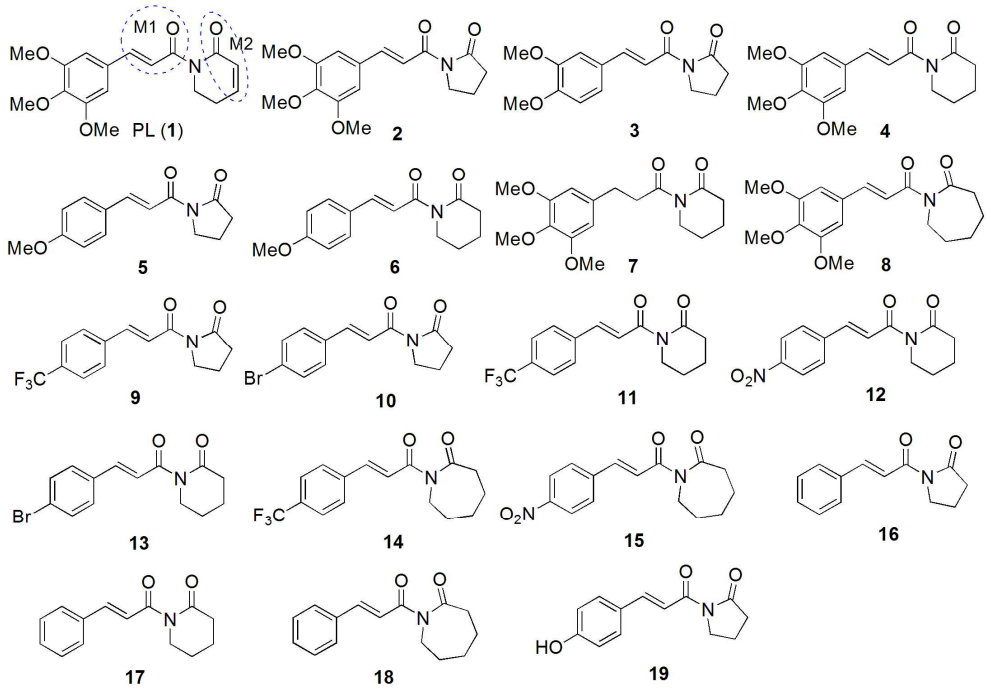

Figure 1. Structures of PL and its analogues.

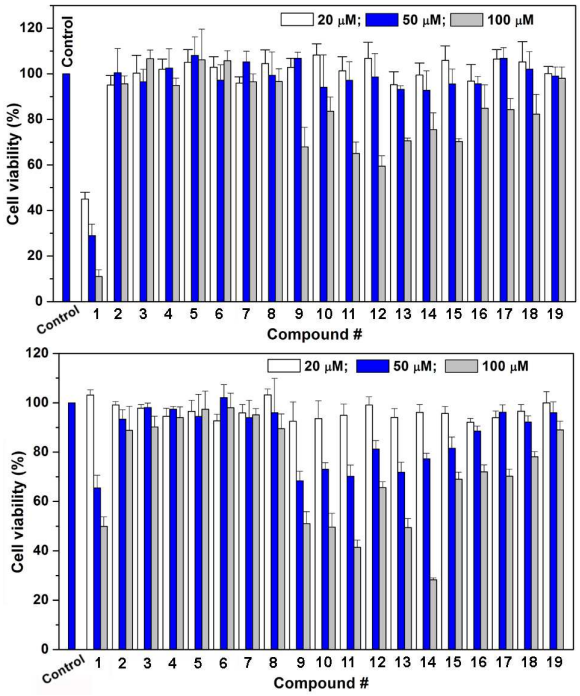

Figure 2. Cytotoxicity screening of PL and its analogues in PC12 cells (A) and L02 cells (B). Cells (1×10^4 cells/well) were plated in a 96-well plate for 1 day and subsequently treated with varying concentrations of drugs, and the cell viability was determined by the MTT assay. All data represent the means ± SD of three independent experiments. *, $P<0.05$, and **, $P<0.01$ vs. the vehicle group.

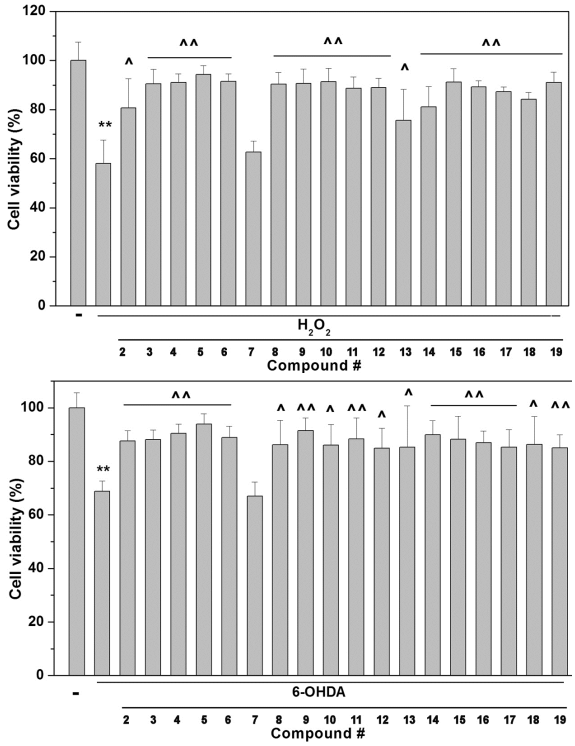

Figure 3. Protection screening of PL analogues against H_2O_2- or 6-OHDA-induced PC12 cell damage. PC12 cells (1×10^4 cells/well) were plated in a 96-well plate for 1 day and subsequently treated with 20 μM drugs for another 24 h. After replacing the medium containing 500 μM H_2O_2 (A) or 200 μM 6-OHDA (B) and continuing incubation for 12 h, the cell viability was measured by the MTT assay. All data represent the means ± SD of three independent experiments. *, $P<0.05$, and **, $P<0.01$ vs. the vehicle group; ^, $P<0.05$, and ^^, $P<0.01$ vs. the H_2O_2- or 6-OHDA-treated group.

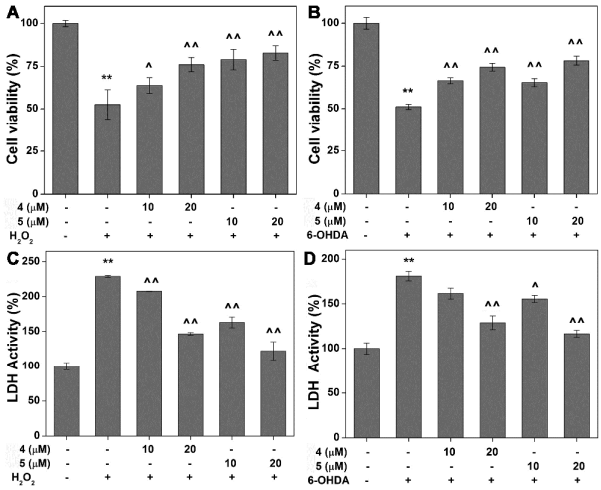

Figure 4. Protection of compounds **4** and **5** against H_2O_2- or 6-OHDA-induced PC12 cell damage. Protection against H_2O_2-induced (A) and6-OHDA-induced (B) PC12 cell damage by the MTT assay. PC12 cells (1×10^4 cells/well) were plated in a 96-well plate for 1 day and subsequently treated with **4** or **5** for another 24 h. After replacing the medium containing 500 μM H_2O_2 or 200 μM 6-OHDA and continuing incubation for 12 h, the cell viability was measured by the MTT assay. Protection against H_2O_2-induced (C) and 6-OHDA-induced (D) PC12 cell damage by the LDH release assay. PC12 cells (1×10^6 cells/well) were seeded in 60-mm dishes for 24 h, and then treated with different concentrations of **4** or **5** for another 24 h. After replacing with the fresh medium containing 500 μM H_2O_2 or 200 μM 6-OHDA and continuing culture for 12 h. The content of LDH in the medium was determined as described in the materials and methods. All data represent the means ± SD of three independent experiments. *, $P<0.05$, and **, $P<0.01$ vs. the vehicle group; ^, $P<0.05$, and ^^, $P<0.01$ vs. the H_2O_2- or 6-OHDA-treated group.

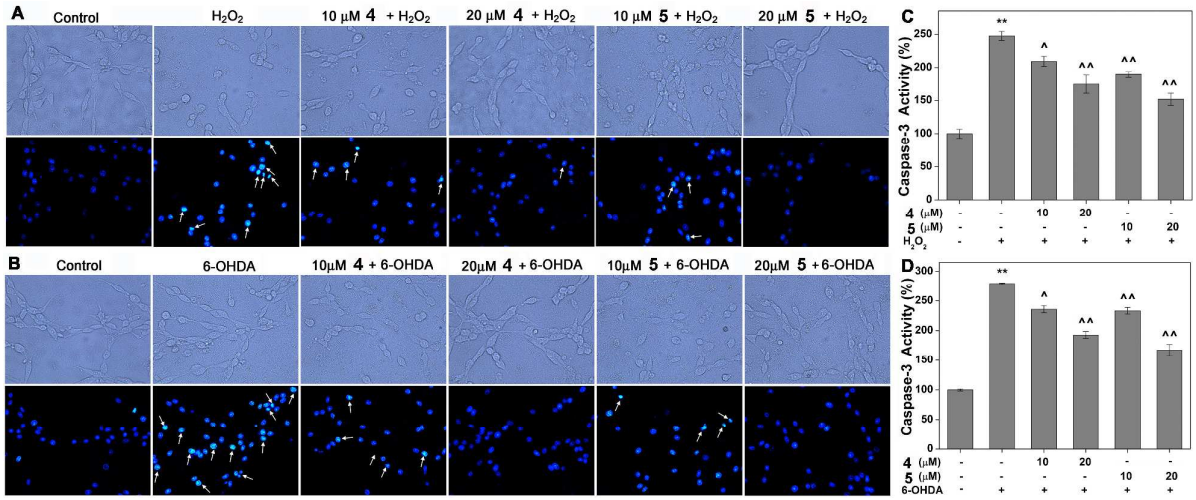

Figure 5. Prevention of PC12 cells from H_2O_2- or 6-OHDA-induced apoptosis by **4** and **5**. (A) & (B) The images show the apoptotic nuclei by Hoechst 33342 staining. Top panel: phase contrast pictures; Bottom panel: fluorescence pictures. (C) and (D) The caspase-3 activity was determined by a colorimetric assay. All data represent the means ± SD of three independent experiments. *, $P<0.05$, and **, $P<0.01$ vs. the vehicle group; ^, $P<0.05$, and ^^, $P<0.01$ vs. the H_2O_2- or 6-OHDA-treated group.

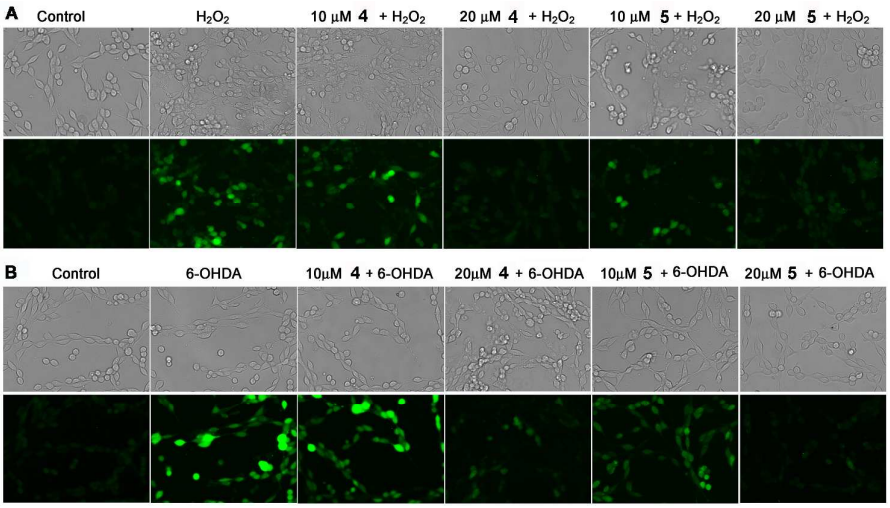

Figure 6. Alleviation of ROS levels in PC12 cells by **4** and **5**. The fluorescence images (bottom panel) demonstrate the prevention of H_2O_2-induced (A) or 6-OHDA-induced (B) ROS accumulation in PC12 cells by **4** and **5**. The corresponding phase contrast images were shown in the top panel.

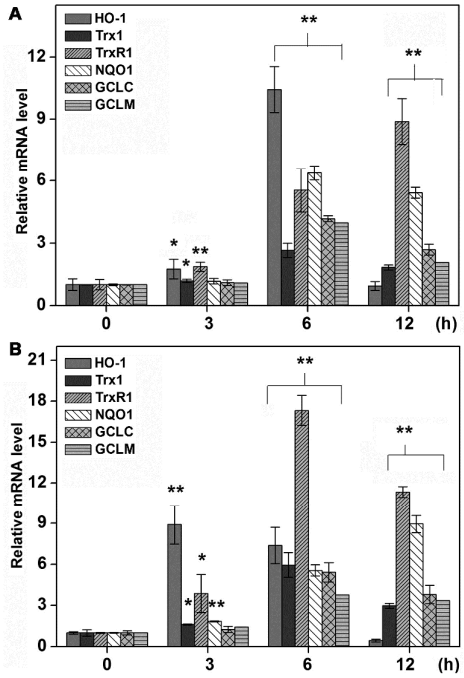

Figure 7. Upregulation of antioxidant genes expression by **4** (A) and **5** (B) in PC12 cells. The expression of different genes was analyzed and normalized using GAPDH as an internal standard by qRT-PCR as described. Data represent the means ± SD of three independent experiments. **, $P < 0.01$ vs. the control group (0 h).

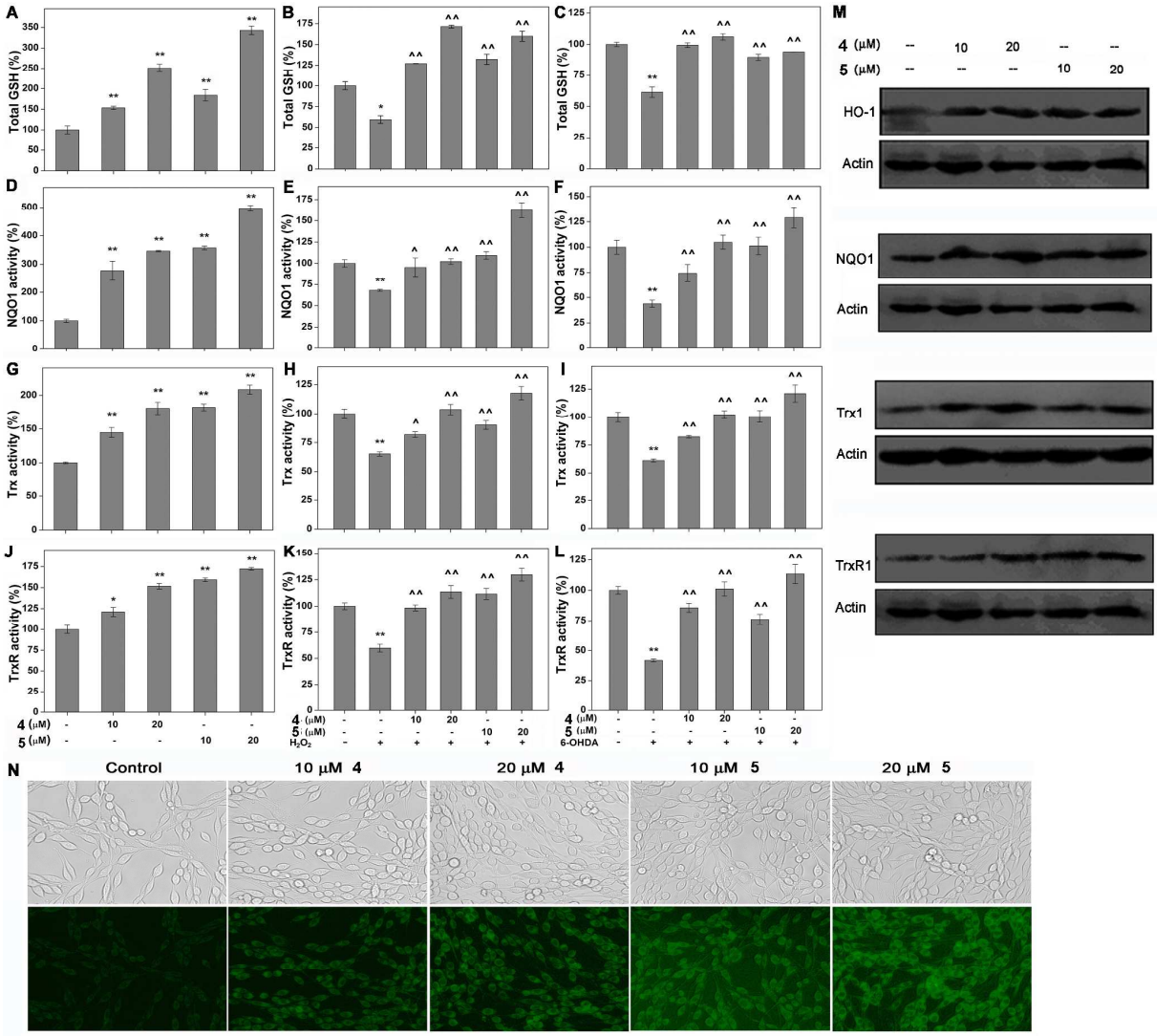

Figure 8. Up-regulation of GSH and antioxidant enzymes by **4** and **5** in PC12 cells. Induction of GSH (A), NQO1 activity (D), Trx activity (G) and TrxR activity (J), and upregulation of the phase II enzymes expression (M). PC12 cells (1×10^6 cells/well) were seeded in 60-mm dishes for 24 h, and treated with **4** or **5** for another 24 h. The GSH levels, and the antioxidant enzymes' activity and expression were determined. Prevention of H_2O_2- or 6-OHDA-induced GSH depletion (B & C), and rescue of NQO1 (E & F), Trx (H & I) and TrxR (K & L) activity by **4** and **5**. The cells (1×10^6 cells/well) were seeded in 60-mm dishes for 24 h, followed by **4** or **5** treatment for another 24 h. After replacing with the fresh medium containing 500 μM H_2O_2 or 200 μM 6-OHDA and continuing culture for 12 h, The GSH levels and the antioxidant enzymes' activity were determined. (N) Detection of the TrxR activity by TRFS-Green in PC12 cells. The phase contrast (top panel) and fluorescence (bottom panel) images were shown. All data represent the means ± SD of three

independent experiments. *, $P<0.05$, **, $P<0.01$ vs. the vehicle group; ^, $P<0.05$, and ^^, $P<0.01$ vs. the H_2O_2- or 6-OHDA-treated group.

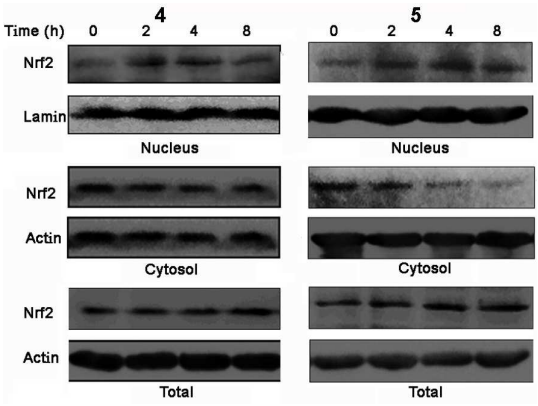

Figure 9. Promotion of Nrf2 nuclear accumulation by **4** and **5**. The PC12 cells (1×10^6 cells/well) were seeded in 60-mm dishes for 24 h, and treated with 20 μM **4** or **5** for 0, 2, 4 and 8 h. Then the cells were harvested and different cell extracts were prepared as described. Nuclear Nrf2, cytosolic Nrf2, and total Nrf2 were analyzed by the Western blots.

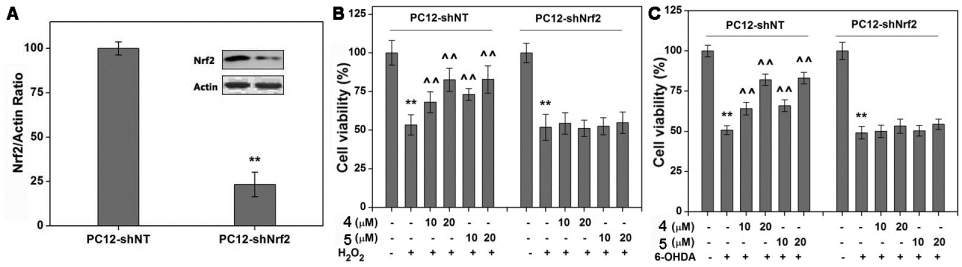

Figure 10. Requirement of Nrf2 for the neuroprotection of **4** and **5** in PC12 cells. (A) Nrf2 expression in PC12-shNT and PC12-shNrf2 cells was determined by the Western blots. The cells (1×10^4 cells/well) were plated in a 96-well plate for 1 day and subsequently treated with **4** or **5** for another 24 h. After replacing the medium containing 500 μM H_2O_2 (B) or 200 μM 6-OHDA (C) and continuing incubation for 12 h, the cell viability was measured by the MTT assay. All data represent the means ± SD of three independent experiments. *, $P<0.05$, **, $P<0.01$ vs. the vehicle group; ^, $P<0.05$, and ^^, $P<0.01$ vs. the H_2O_2- or 6-OHDA-treated group.

Table of Contents graphic (13.5 x 5.5 cm)